Technical feasibility of a Dutch radioactive waste repository in Boom Clay: Thermo-hydro-mechanical behaviour

OPERA-PU-TUD321c

Radioactive substances and ionizing radiation are used in medicine, industry, agriculture, research, education and electricity production. This generates radioactive waste. In the Netherlands, this waste is collected, treated and stored by COVRA (Centrale Organisatie Voor Radioactief Afval). After interim storage for a period of at least 100 years radioactive waste is intended for disposal. There is a world-wide scientific and technical consensus that geological disposal represents the safest long-term option for radioactive waste.
Geological disposal is emplacement of radioactive waste in deep underground formations. The goal of geological disposal is long-term isolation of radioactive waste from our living environment in order to avoid exposure of future generations to ionising radiation from the waste. OPERA (OnderzoeksProgramma Eindberging Radioactief Afval) is the Dutch research programme on geological disposal of radioactive waste.
Within OPERA, researchers of different organisations in different areas of expertise will cooperate on the initial, conditional Safety Cases for the host rocks Boom Clay and Zechstein rock salt. As the radioactive waste disposal process in the Netherlands is at an early, conceptual phase and the previous research programme has ended more than a decade ago, in OPERA a first preliminary or initial safety case will be developed to structure the research necessary for the eventual development of a repository in the Netherlands. The safety case is conditional since only the long-term safety of a generic repository will be assessed. OPERA is financed by the Dutch Ministry of Economic Affairs, Agriculture and Innovation and the public limited liability company Electriciteits-Produktiemaatschappij Zuid-Nederland (EPZ) and coordinated by COVRA. Further details on OPERA and its outcomes can be accessed at www.covra.nl.

This report concerns a study conducted in the framework of OPERA. The conclusions and viewpoints presented in the report are those of the author(s). COVRA may draw modified conclusions, based on additional literature sources and expert opinions. A .pdf version of this document can be downloaded from www.covra.nl

OPERA-PU-TUD321c
Title: Technical feasibility of a Dutch radioactive waste repository in Boom Clay: Thermo-hydro-mechanical behaviour
Authors: Philip J. Vardon, Poly Buragohain, Michael A. Hicks, Jaap Hart, Peter A. Fokker and Caroline C. Graham.
Date of publication: June 2017
Keywords: Boom Clay, thermo-hydro-mechanical, feasibility.

TU Delft

Technical feasibility of a Dutch radioactive waste repository in Boom Clay: Thermo-hydro-mechanical behaviour

June 2017

Philip J. Vardon[1], Poly Buragohain[1], Michael A. Hicks[1], Jaap Hart[2], Peter A. Fokker[3] and Caroline Graham[4]

[1] Delft University of Technology (TUD), Geo-Engineering Section, Delft
[2] Nuclear Research and Consultancy Group (NRG), Petten
[3] Nederlandse Organisatie voor Toegepast Natuurwetenschppelijk Onderzoek (TNO), Utrecht
[4] British Geological Survey (BGS), Keyworth

Contents

Summary

The *Onderzoeks Programma Eindberging Radioactief Afval* (OPERA) is the third national research programme for the geological disposal of radioactive waste in the Netherlands, operating during the period 2011 to 2016. This document reports part of Work Package 3.2.1, where a number of aspects related to the technical feasibility were investigated.

This report presents a study of the thermo-hydro-mechanical behaviour of the proposed Dutch radioactive waste repository. The main objective is to address the technical feasibility of the repository and to highlight key factors which need to be taken into account in the detailed design and in further experimental and numerical studies.

A selective literature study, designed to complement more general literature studies is presented with a focus on understanding the observed Boom Clay behaviour and including it within numerical modelling. A compilation of key parameters is given, showing the range of data available.

A numerical modelling investigation is then presented. The pore pressure is greatly affected by the heat output and the low permeability of the Boom Clay, which then causes a development of the plastic zone in the Boom Clay. The development of the plastic zone typically causes increased loads onto the tunnel liner and this should be included in the detailed design. The plastic zone may cause an increase in permeability as the clay fabric is damaged, although the impact of this is not easily quantified using current information. It is of importance in the overall performance of the repository, with regard to restricting flow around the repository.

This plastic zone is seen, via a sensitivity analysis, to be greatly affected by the thermal expansion of the Boom Clay. This parameter has been extracted from experimental data, but is affected by plasticity, boundary conditions and stress history and therefore is a key parameter to measure more clearly. Conversely, the heat output evolution, i.e. how the heat output reduces in time, of the waste is also not well known, and therefore should be further clarified. This means that, if the performance assessment and detailed design require the plastic zone to be limited in extent, the spacing of the waste packages can be used to control this zone.

Samenvatting

OnderzoeksProgramma Eindberging Radioactief Afval (OPERA) is het derde nationale onderzoeksprogramma naar geologische eindberging in Nederland, uitgevoerd in de periode tussen 2011 tot 2016. Dit document betreft werkpakket 3.2.1, waar een aantal aspecten gerelateerd aan de technische haalbaarheidsstudie zijn onderzocht.

Dit rapport betreft een studie naar het thermo-hydro-mechanische gedrag van de voorgestelde Nederlandse eindberging voor radioactief afval. De hoofddoelstelling is de technische haalbaarheid van de eindberging te toetsen en van sleutelfactoren te identificeren die in rekening gebracht dienen te worden bij experimentele en numerieke vervolgstudies.
Een selectieve literatuurstudie is uitgevoerd, met als doel het algemene literatuuroverzicht betreffende het materiaalgedrag van boomklei aan te vullen en deze aanvullingen mee te nemen in de numerieke modellen. Een samenvatting van belangrijkste parameters is gegeven, waarin de spreiding van de data wordt gepresenteerd.

Dit rapport presenteert onderzoeksresultaten van numerieke simulaties. Deze resultaten tonen aan dat de waterspanning sterk wordt beïnvloed door de gegenereerde warmte en de lage doorlatendheid van de Boomse klei. Dit resulteert vervolgens in een vergroting van de plastische zone in de Boomse klei. Een typische reactie van een vergroting van de plastische zone is een verhoogde spanning op de tunnel-liner en dit dient in het gedetailleerde ontwerp meegenomen worden. De plastische zone kan leiden tot een verhoging van de doorlatendheid zodra de kleistructuur wordt beschadigd. De impact hiervan is echter niet zomaar te kwantificeren aan de hand van de huidig beschikbare informatie. Het nader bepalen van deze impact is een belangrijk punt in de evaluatie van de algemene prestatie van de eindberging, met betrekking tot het beperken van de stroming langs de eindberging.

Uit de gevoeligheidsanalyse blijkt dat de plastische zone sterk beïnvloed wordt door de thermische expansie van de Boomse klei. Deze uit experimentele data verkregen parameter wordt beïnvloed door de plasticiteit, de randvoorwaarden en het spanningsverleden en is hierdoor een belangrijke parameter om nauwkeurig te meten. Anderzijds is de evolutie van de gegenereerde warmte (d.w.z. hoe de gegenereerde warmte van het radioactief afval verminderd in tijd) ook niet goed bekend en dient verdere specificatie. Dit betekent dat, als de toetsing van de prestatie en het gedetailleerde ontwerp een gelimiteerde plastische zone vereisen, de afstand tussen de containers voor radioactief afval gebruikt kan worden om deze zone te controleren.

Notation

This list contains definitions of acronyms and symbols including dimensions. All symbols are also defined in the text of the report. The dimensions are defined in typical SI units.

Symbol	Definition	Unit
Acronyms		
BGS	British Geological Survey	
CERBERUS	Control Experiments with Radiation of the Belgian Repository for Underground Storage	
HS	Hardening Soil	
OCR	Over-Consolidation Ratio	
OPERA	Onderzoeksprogramma Eindberging Radioactief Afval	
NRG	Nuclear Research and Consultancy Group	
SAFIR	Safety Assessment and Feasibility interim Report 2	
THM	Thermo-Hydro-Mechanical	
TIMODAZ	Thermal Impact on the Damage Zone around a Radioactive Waste Disposal in Clay Host	
TNO	Nederlandse Organisatie voor Toegepast Natuurwetenschappelijk Onderzoek	
TUD	Delft University of Technology	
Greek letters		
α	Thermal diffusivity	[$m^2 s^{-1}$]
α_s	Linear thermal dilation or expansion coefficient	[K^{-1}]
β_T	Thermal compressibility coefficient (volumetric)	[K^{-1}]
β_{wP}	Compressibility of water	[Pa^{-1}]
β_{wT}	Thermal expansion of water	[Pa^{-1}]
$\boldsymbol{\varepsilon}$	Strain tensor	[-]
$\boldsymbol{\varepsilon}_T^e$	Thermally induced elastic strain tensor	[-]
λ	Thermal conductivity	[$W\ m^{-1} K^{-1}$]
Λ	Thermal pressurisation coefficient	[$Pa\ K^{-1}$]
μ	Viscosity	[$N\ s\ m^{-2}$]
ν	Poisson's ratio	[-]
ρ	Density	[$kg\ m^{-3}$]
$\boldsymbol{\sigma}$	Total stress tensor	[Pa]
$\boldsymbol{\sigma}'$	Effective stress tensor	[Pa]
ϕ	Effective friction angle	[°]
ψ	Dilatancy angle	[°]
Latin letters		
C	Specific heat capacity	[$J\ kg^{-1} K^{-1}$]
c	Volumetric heat capacity	[$J\ m^{-3} K^{-1}$]
c	Cohesion	
E_{50}^{ref}	Reference secant modulus	[Pa]
E_{oed}^{ref}	Reference oedometer modulus	[Pa]
E_{ur}^{ref}	Reference un/reloading modulus	[Pa]
e	Void ratio	[-]
g	Gravitational constant	[$m\ s^{-2}$]
$\mathbf{g}$	Gravitational matrix	[$m\ s^{-2}$]
J	Heat flux	[W]

K	Hydraulic conductivity	[m s^{-1}]
K_0	At rest earth pressure	
k	Permeability	[m^2]
$\mathbf{M}$	Material matrix	[Pa]
m	Rate of stress dependency of stiffness	[-]
$\mathbf{m}$	Identity matrix	[-]
n	Porosity	[-]
p'	Mean effective stress	[Pa]
p_c	Cavity pressure	[Pa]
p^{ref}	Reference stress	[Pa]
p_w	Pore water pressure	[Pa]
Q_T	Heat source (or sink)	[J]
Q	Deviatoric stress	[Pa]
R_f	Reference stress	[Pa]
r	Radius	[m]
T	Temperature	[K]
t	Time	[s]
V	Volume	[m^3]

Sub- and superscripts

0	Initial conditions
c	Conductive
HZ	Hardening zone
h	Horizontal
max	Maximum
p	Pressure
s	Solid
T	Temperature
ur	Unload/reload
v	Vertical
w	Water

1. Introduction

This report is part of an investigation into the principle feasibility of a deep geological repository for radioactive waste in the Netherlands. This work is undertaken as part of the Onderzoeksprogramma Eindberging Radioactief Afval (OPERA) research programme in Work Package (WP) 3.2.1. This report follows from WP 3.1, where a number of additional aspects relating to the principle feasibility were identified for further investigation. The results of WP 3.2.1 are presented in the following reports:

- Yuan, J., Vardon, P.J., Hicks, M.A., Hart, J., Fokker, P.A. (2016) *Technical feasibility of a Dutch radioactive waste repository in Boom Clay: Plugs and seals*. OPERA-PU-TUD321a.
- Yuan, J., Vardon, P.J., Hicks, M.A., Hart, J., Fokker, P.A. (2016) *Technical feasibility of a Dutch radioactive waste repository in Boom Clay: Tunnel crossings*. OPERA-PU-TUD321b.
- Vardon, P.J., Buragohain, P., Hicks, M.A., Hart, J., Fokker, P.A., Graham, C.C. (2016) *Technical feasibility of a Dutch radioactive waste repository in Boom Clay: Thermo-hydro-mechanical behaviour* OPERA-PU-TUD321c.
- Li, Y., Vardon, P.J., Hicks, M.A., Hart, J., Fokker, P.A. (2016) *Technical feasibility of a Dutch radioactive waste repository in Boom Clay: Geomechanical validation.* OPERA-PU-TUD321d.

The main objective of this report is to investigate and analyse the thermo-hydro-mechanical (THM) phenomena in Boom Clay for the proposed Dutch radioactive waste repository. In this research, the numerical analysis is being carried out by the numerical code PLAXIS developed by Plaxis (2015). The research was undertaken by Delft University of Technology (TUD), Nuclear Research and Consultancy Group (NRG), Nederlandse Organisatie voor Toegepast Natuurwetenschappelijk Onderzoek (TNO) and the British Geological Survey (BGS) during the period from 5-2015 till 6-2016.

1.1. Background

Final disposal of radioactive waste in deep geological formations is proposed as the most likely options for the Netherlands and also worldwide. In this concept of the geological disposal system, Boom Clay is considered as a potential host formation in the Netherlands. A limited amount of waste in the Netherlands is considered to be heat producing, although it is this waste which is the most radioactive.

Transient elevated thermal behaviour has a number of associated effects, including pore pressure rise, thermal expansion, and even changes in the mineralisation of the clay structure. These can then give rise to changes in properties that affect the performance of the repository, e.g. hydraulic and mechanical properties. Note that these effects are different for other host rock types.

An initial scoping investigation of the temperature evolution of the proposed OPERA repository (Verhoef, 2014) was carried out in WP3.1 (Arnold et al., 2015) and concluded that the temperature values yielded were likely to be significantly below any limiting values, but it was recommended that coupled behaviour, i.e. Thermo-Hydro-Mechanical-Chemical behaviour, be investigated. It was shown that the long-term storage proposed in the Netherlands significantly reduces the heat output of the waste, which leads to relatively moderate calculated temperature increases. In this work, the coupled behaviour is investigated.

Various coupled mechanical (M), hydraulic (H) and thermal (T) perturbations will be induced in the surrounding clay host rocks and create a disturbed zone, due to first the tunnel construction, and then the heat from waste which must dissipate through the host rock. The heat flow generally takes place by conduction (Fourier's law) and by convection with water flow, but given the very weak flow rate this mode can be considered negligible. Generally, when the temperature increases there is also an increase in the water volume and in the pressure in the host rock. Pore pressures are dissipated via advective flow which is limited by the very low hydraulic conductivity of the host rock, and which in turn affects the mechanical behaviour.

This project investigates the major coupled thermal–hydraulic–mechanical (THM) processes in the clay host rock in the proposed OPERA repository.

1.2. Objectives

The objectives of this report are:

- To provide a selective review of the existing knowledge and observations (both laboratory and in situ) regarding the THM behaviour in clays, especially Boom Clay, in the context of radioactive waste disposal. The review will focus on the significant temperature-dependent material properties and coupled processes and parameters for the hydro-mechanical response of the Boom Clay and will focus on the integration into computational analysis;
- To assess the consequence of the heat generated by the radioactive waste on the performance of the proposed disposal system;
- To assess the sensitivity of the response with respect to variable parameters in a quantitative manner.

1.3. Scope of this research

The scope of this research is as follows:

- The work was limited to Boom Clay as the host rock;
- The assessment of the THM behaviour was based on the current knowledge and available material data from the literature.
- The Hardening Soil (HS) model for modelling of the THM behaviour of the Boom Clay was utilised (see Arnold et al., 2015 for detailed reasoning).
- No chemical, gas or biological impacts are considered.

1.4. Outline of the report

This report is divided into five chapters and contains one appendix. Chapter 2 provides a selective literature review on various aspects of the THM behaviour for deep geological disposal, aiming to provide background for the development of a technically feasible Dutch radioactive waste repository in Boom Clay. Chapter 3 provides the set-up of the numerical model, including the theory and governing equations for the THM simulations, the domain and simulation strategy. Chapter 4 presents a detailed study on the simulation results conducted using the finite element code PLAXIS (Plaxis, 2015). A variety of analyses are presented with three sets of thermal conditions (extreme, low and medium) to determine the evolution of temperature, pore pressure, stress/strain, displacement in the Boom Clay. In particular, the plastic zone and the stress paths have been assessed. Mechanical, hydraulic and thermal sensitivity analysis has been performed by varying individual model parameters and boundary conditions, to assess their impact on the extent of the plastic zone and the liner forces in chapter 5. The analyses provide insight into the significance of these variables on the analysed coupled processes. A summary, conclusions and some recommendations for further work is presented in Chapter 6.

2. Selective literature review

2.1. Introduction

This chapter presents an overview of the existing literature on thermal-hydraulic-mechanical (THM) behaviour related to the behaviour of clays during the disposal of heat emitting radioactive waste. The major emphasis is on Boom Clay, yet some results pertain to rocks, clays, volcanic tuff and other materials, where relevant phenomena are observed in these materials.

Both material properties and processes are detailed to clarify the thermal impact on them and therefore the possible impact on performance and safety. The focus is on the ability to simulate the processes computationally to inform following analyses. A review of the Boom Clay properties and behaviour is given by Arnold et al., (2015) and Wiseall et al. (2016) and this focused review complements these reports. This review differs by the focus being on the immediate post operation phase, on thermal impacts on the THM behaviour and, in particular on the phenomena included in the modelling formulation utilised and the calibrated constitutive model.

2.2. Background

There are many functions of the multi-barrier system in radioactive waste disposal with regard to both mechanical and hydraulic properties. The two basic functions of the barrier materials are as follows: (i) the materials should structurally hold the radioactive waste canisters in place and prevent collapse of the excavation; and (ii) the materials should create a very high level of water tightness to limit the access of water to the waste containers in order to prevent migration of radionuclide into the geosphere. These should function as long as is required (Smith et al., 2009). While there is no specific safety function regarding heat or temperature (Smith et al., 2009; Hart and Poley, 2014) it should not unduly impact the above functions, and therefore the barrier material should transfer the heat generated in the waste away from the near field. During the operational phase, the near field is expected to be challenged by conditions of high temperature and hydraulic pressure.

A significant challenge in repository design is predicting the long-term thermal effects and behaviour of heat-emitting radioactive waste and numerous research has been conducted (e.g. Sillen and Marivoet 2007; Chen et al. 2011; Yu et al., 2014; Thomas et al., 2014). It can be noted that, because of the heat output, the waste cannot be placed in a repository immediately after extraction from a reactor but is generally recommended to be stored for some tens of years in temporary storage before disposal. For the Netherlands the interim storage period is at least 100 years (Verhoef et al., 2014).

The heat and temperature resulting after emplacement of heat-producing waste in the geological disposal facility, after the cooling-down period, will still have an impact on both the near field and the far field (SAFIR 2 project; ONDRAF/NIRAS 2001a, b). In the near field, the heating may alter the physicochemical properties of the waste, the backfill material, and the structural material of the disposal galleries, as well as increase the corrosion rate of the packaging materials. Whereas in the far field, heating could alter the geochemical, geomechanical, and hydrogeological conditions in the clay as well as its mineralogy (Baldi et al., 1988; Hueckel and Baldi, 1990; De Bruyn and Thimus, 1996; Delage et al., 2000; Cui et al., 2000; Sultan et al., 2002, Cui et al., 2009, François et al., 2009). It could also modify the hydrogeological regime in the adjacent aquifers (Van Marcke and Laenen 2005). Thus these impacts could have repercussions for the entire design of the repository (Wang et al. 1988; Goblet 2000).

Numerous studies have investigated the thermo-hydro-mechanical behaviour of geological formations for radioactive waste disposal (Horseman et al., 1987; Baldi et al., 1988, 1991a,b; Sultan, 1997; Sultan et al., 2002; Coll, 2005; Deng et al., 2011a, 2011b, 2012).

Over the past decades various studies on the development of computer simulation programs for analysing the coupled THM behaviour of clay buffers and backfill, in various disposal concepts and host rocks/clays, has been carried out (Noorishad et al., 1984; Thomas and He, 1998; Olivella et al., 1995; Rutqvist et al., 2001). Further work is supported with the validation and application of the developed programs using laboratory and in situ tests (Onofrei and Gray, 1996; Chandler et al., 1998; Chijimatsu et al., 2001; ENRESA, 2000; Collin et al., 2002; Olivella and Gens, 2005; Thomas et al., 2014).

However, there are fewer studies examining time dependent thermal effects on Boom Clay behaviour, which limits a thorough analysis of the long-term behaviour of the radioactive disposal facility. A good comprehension of the processes which occur during the heat-emitting stage of thermal transient is pivotal. Some of the properties include a very low permeability, the absence of preferential migration pathways for solutes, swelling and creep properties.

For Boom Clay, the major impacts of the short term thermal behaviour are anticipated to be:

- The additional mechanical loads that are imposed on the lining;
- Changes in pore pressure around the disposal gallery, altering the mechanical behaviour of the Boom Clay;
- Mechanical damage and consequential changes in hydraulic conductivity around the tunnels.

In the Netherlands, the amount of heat-generating waste is relatively small and is proposed to be in the disposal galleries located off the large curved part of the main gallery, shown in Figure 2.1. It is seen that this part is a relatively small part of the repository.

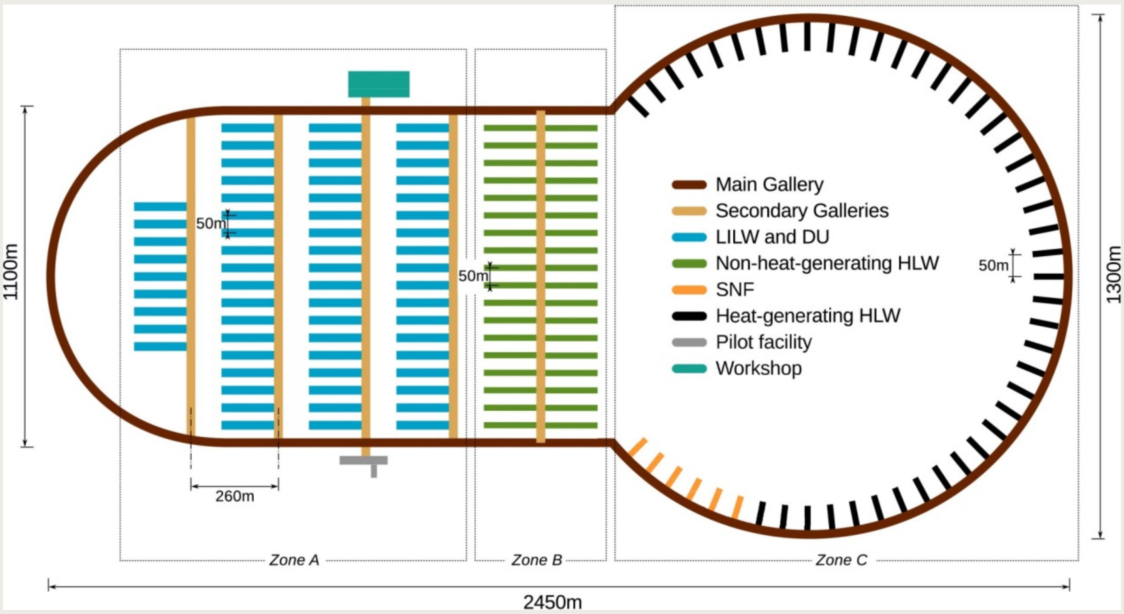

Figure 2.1.: Repository layout (after Verhoef et al., 2014).

2.3. Limiting temperatures

There is no specific temperature value or limit which is associated with endangering the safety of the repository. The temperature, as with all other aspects, is required to not unduly affect the safety functions of the repository.

SAFIR 2 (Section 11.3.7.3 ONDRAF/NIRAS 2001b) has recommended the following maximum allowable temperatures: for the vitrified waste, 400°C, which is 100°C below the temperature above which the structure of the matrix alters and its mechanical properties change; for the spent fuel assemblies, 350°C, to prevent an excessive pressure build-up by the helium present in the fuel rods; for the backfill material, 100°C, to prevent any physico-chemical alteration of the material and, in particular, to prevent any significant disturbance of the local hydraulic system following the increase in pore pressure.

The maximum allowable temperature increase for the clay has been proposed to be about 85°C, in order not to exceed 100°C, based on the initial temperature of 16°C (ONDRAF/NIRAS 2001b). This limit was based on an observed maximum temperature observed during the CERBERUS experiment of 100°C, where no significant change in the properties of the clay could be demonstrated. However, it should be noted that this experiment was conducted under 'Mol conditions', not at depths relevant for the Netherlands.

2.4. Evolution of Temperature

The evolution of the temperature field around the repository system is an essential input to many phenomenological studies, which can lead to alteration of the system which may affect safety. The initial state and ability of heat to move through the system govern its evolution.

2.4.1. Initial state

The ambient temperature can vary significantly from site to site. At a depth of 500m an average temperature of about 20-25°C is reported in Belgium, that is, with local anomalies ranging from 15°C to 30°C (Vandenberghe and Fock, 1989). A temperature map of the Dutch subsoil at a depth of 500m was presented by Rijkers et al. (1998). This shows a similar trend with temperatures varying between 20°C and 30°C. At a depth of 1000m, significantly higher temperatures are observed, ranging from 40°C to 55°C, with a larger spatial variation. The geothermal gradient up to a depth of 1000m was defined by (ONDRAF/NIRAS, 2001a) to be 3.5°C per 100m.

2.4.2. Transport mechanism

The low permeability of clay ensures that the heat transport mechanism is governed by heat conduction and that advection (convective flux) is negligible (Gens et al., 2009). Conservation of energy and Fourier's law form the governing equation (e.g. Arnold et al., 2015):

$$\frac{\partial T}{dt}(C\rho) = \nabla(\lambda \nabla T) + Q_T \tag{2-1}$$

where T is the temperature, t is the time, C is the specific heat capacity, ρ is the density, λ is the thermal conductivity and Q_T is a heat source (or sink). The specific heat capacity, density and thermal conductivity are typically defined using mixture theory based upon the solid and water content of the material, either using the geometric or arithmetic means (e.g. Arnold et al., 2015; Wiseall et al., 2016). The specific heat capacity, density and thermal conductivity are often combined into a single parameter called the thermal diffusivity ($\alpha = \lambda / C\rho$), and the specific heat capacity and density combined into the volumetric heat capacity($c = C\rho$).

Table 2.1 summarises some ranges of thermal soil property values obtained from the very limited amount of data available in the literature. Moreover, a difference in the vertical and horizontal thermal conductivities is evident (e.g. Garitte et al., 2012). Similarly, the difference in temperature increase measured during the ATLAS III heater test between a horizontal and an inclined observation borehole, that is, with both having the same distance to the heater, is clear evidence for an anisotropic thermal conductivity in the Boom Clay (Chen et al., 2011). Recently, Garitte et al. (2012) characterised the thermal conductivity of three argillaceous rocks, i.e. Callovo-Oxfordian Clay, Opalinus Clay and Boom Clay, on the basis of temperature measurements in the rock mass of four in situ heating experiments as well as results from the laboratory. The laboratory results were found to closely agree with the data obtained in the field. A set of reference thermal conductivity values for all three host rocks was proposed, all of which are anisotropic in nature. The thermal conductivity in the Boom Clay was found to be lower than in the two indurated rocks.

2.5. *Thermal effects on hydraulic behaviour*

2.5.1. Volumetric response (thermal expansion / pore pressure generation)

As the temperature changes, the volume of the (pore) water also changes. Above around 4°C the volume increases with increased temperature, i.e. the density decreases. This rate is non-linear over a significant temperature range (Kaye and Laby, 1973), but can be typically defined by a linear coefficient of thermal expansion (e.g. Wiseall et al., 2016), which may be updated with temperature and pressure, e.g.

$$\beta_T = \frac{1}{V}\left(\frac{\partial V}{\partial T}\right)_p = -\frac{1}{\rho}\left(\frac{\partial \rho}{\partial T}\right)_p \tag{2-2}$$

where V is the volume and the subscript p relates to constant pressure. For water, $\beta_{wT} \approx 2.1 \times 10^{-4}\ °C^{-1}$ at atmospheric pressure and 20°C.

In a porous medium, e.g. a clay, the water is not totally free to expand, and therefore the compressibility (Kaye and Laby, 1973) and confining conditions also govern the behaviour. The compressibility is again non-linear over a large pressure range, but can be assumed constant within a limited pressure range. The water density can be calculated by use of (Rutqvist et al., 2001; Plaxis 2015):

$$\frac{\rho_w}{\rho_{w0}} = 1 - \beta_{wP}(p_w - p_{w0}) - \beta_{wT}(T - T_0) \tag{2-3}$$

where ρ_w is the density of water, p_w is the pore water pressure, β_{wP} is the compressibility of water, β_{wT} is the thermal expansion of water and the subscript 0 relates to the initial condition.

The flow of water, i.e. the ability for pressure to dissipate, is defined typically via Darcy's Law which is not covered explicitly here. Coupling of the pressure changes and the mechanical component have been dealt with in section 2.7.

2.5.2. Permeability and hydraulic conductivity

The intrinsic permeability of a material is fluid independent and is related to the hydraulic conductivity via the fluid properties as:

$$K = \frac{k\rho g}{\mu} \tag{2-4}$$

where K is the hydraulic conductivity, k is the intrinsic permeability, g is the gravitational constant and μ is the viscosity. The viscosity (and density) of water is temperature dependent and can be approximated via (Kaye and Laby, 1973):

$$\mu = 661.2(T + 44.15)^{-1.562} \times 10^{-3} \pm 0.5\%\ (Ns/m^2) \tag{2-5}$$

There are very limited tests to investigate the impact of temperature on permeability and even fewer when considering Boom Clay. A body of work examining the hydraulic conductivity of clays exists, based upon isothermal consolidation tests performed at various temperatures (Sultan, 1997; Habibagahi 1977; Morin and Silva 1984; Towhata et al. 1993). A change in consolidation coefficient and hydraulic conductivity is observed with temperature, although these variations could be explained via changes in fluid properties.

As stated by Wiseall et al. (2016), tests undertaken by Delage et al. (2000) and during the TIMODAZ project showed no significant changes in intrinsic permeability with temperature (up to 80°C). Increases of hydraulic conductivity were observed with temperature, but returned to the initial value after cooling. This was attributed to the reversible decreases in water viscosity (Delage et al. 2000; Chen et al. 2014) and it was concluded that no change in the pore structure was apparent.

Further, in tests on fractured samples the permeability also seemed to be unaffected, with only one drained shearing test with a low mean stress yielding a significant increase in permeability (Delage, 2010).

However, the permeability is likely to be affected by changes in volume, which could be caused by changes in temperature. As temperature is concluded to not change the pore structure itself, this is likely to be related uniquely to the density. Morin and Silva (1984) reported that for various clays there is an unique and linear relationship between the porosity and the logarithm of the intrinsic permeability. As reported by Wiseall et al. (2016), Volckart et al. (1995) showed the relationship between hydraulic conductivity and effective stress to exhibit hysteresis, similar to that of void ratio and effective stress, supporting the hypothesis of a unique relationship between porosity (or other volume measure) and permeability.

2.6. *Thermal effects on mechanical behaviour*

2.6.1. Volumetric response (expansion and contraction)

The experimentation into the volumetric response due to temperature of saturated clays is challenging due to the co-generation of pore pressure. This leads to the observed responses being affected strongly by the boundary conditions and rates of loading (Wiseall et al., 2016). A detailed review into the individual experiments is presented by Wiseall et al. and is therefore not repeated here.

Physically, unconfined saturated clays expand when heated. As the thermal expansion coefficient of water is much larger than that of the surrounding soil skeleton, the resulting restriction on water expansion yields an increase in pore water pressure (Britto et al. 1989).

Hueckel and Baldi (1990), Baldi et al. (1991a,b) and Sultan et al. (2002) found that the thermal behaviour of the Boom Clay is characterised by nonlinear and irreversible volume changes that significantly depend on the over-consolidation ratio (OCR), see Figure 2.2. Low OCR values promote irreversible thermal contraction, while high OCR values give reversible thermal dilation. The volume change behaviour was observed to be time dependent and governed by the stress level and temperature. Over-consolidated samples submitted to a slow temperature elevation in drained conditions (with no pore water pressure changes) first exhibited thermal dilation followed by an irreversible plastic contraction. Dilation was observed when heating the soil at low isotropic stresses or high over-consolidation ratios (OCR). However, when heating was introduced at high isotropic stresses (or low OCRs), dilation was induced first, followed by contraction. Hueckel and Pelligrini (1992) found that the volumetric changes could be satisfactorily explained via the effective stress principle, and a thermo-elasto-plastic model with a thermally controlled yield surface. François et al. (2009) successfully calibrated thermal dilation and contraction at differing OCR utilising the same parameter set for such a model.

Sultan et al. (2002) concluded that, (i) the plastic contraction of normally consolidated Boom Clay samples is independent of the applied mean effective stress, (ii) the thermal contraction increases with decreasing OCR values until pure contraction at OCR = 1, (iii) the slope of the volumetric strain during cooling is independent of the mean effective stress applied, and (iv) the temperature at which expansion transits to contraction is associated with a decreasing OCR (Figure 2.2(b)).

A physical explanation of the behaviour was given by Cui et al. (2009) that thermal expansion can be described by the thermal dilation of the solid and fluid phases, whereas the explanation of the plastic thermal contraction is associated with the separation of the adsorbed water from the clay particles requiring physio-chemical interactions between the molecules.

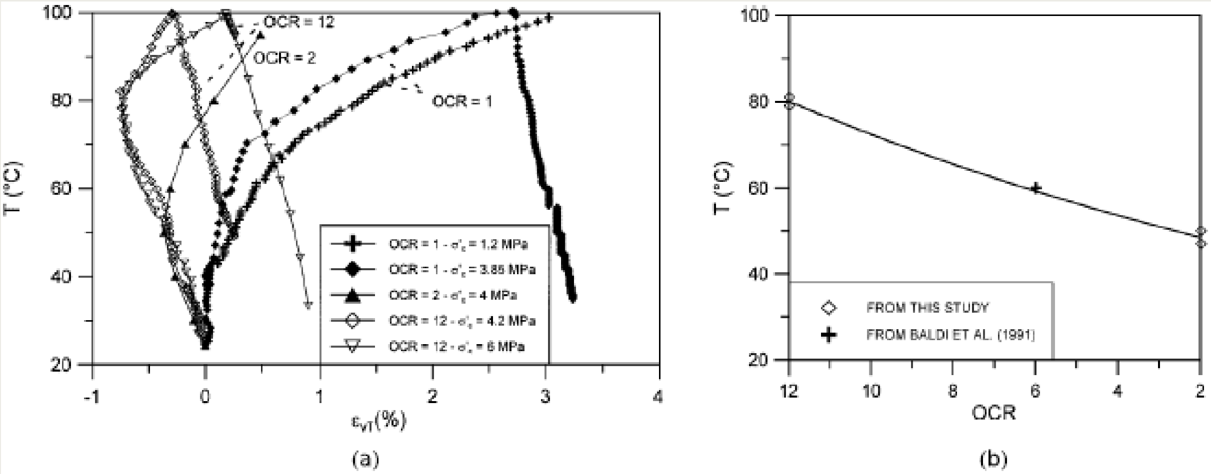

Figure 2.2.: (a) Thermal volumetric changes of Boom Clay samples at different OCRs. (b) Change of the temperature of the thermal expansion/contraction transition as a function of OCR (Sultan et al., 2002).

Elastic deformation

Thermally induced elastic deformation in Boom Clay has been shown to be controlled by a constant linear parameter (François et al. 2009):

$$d\boldsymbol{\varepsilon}_T^e = \alpha_s \mathbf{m} dT \tag{2-6}$$

where $\boldsymbol{\varepsilon}_T^e$ is the thermally induced elastic strain, α_s is the linear thermal dilation or expansion coefficient (note that this is 3 times smaller than the volumetric expansion coefficient, both of which are quoted in literature) and m is the identity matrix (implying that the strain is isotropic). Reported values are given in Table 2.1. It is clear that there is a rather large range of suggested values between 5×10^{-5} and 5×10^{-6} K^{-1}, which could be due to the boundary conditions of the tests or the variability and stress history of the material.

Compressibility

Delage et al. (2010) highlight that, while early studies showed differences in elastic and plastic compression due to temperature and in pre-consolidation pressure, other studies only show differences in plastic yield (discussed below) and not in compressibility. The calculation from experiments carried out (Delage et al., 2010) support this observation. However, both Sultan et al. (2002) and Le (2008) show moderate differences in volume change coefficients with temperature.

Plastic yield: isotropic behaviour

By compiling results from studies on the consolidation of five different clays, Cekerevac and Laloui (2004) showed that the pre-consolidation pressure, i.e. the pressure where a transition from elastic to plastic behaviour occurs, decreases with increasing temperature. Figure 2.3 shows this behaviour for a range of clays (Fig. 2.3a) and for Boom Clay (Fig. 2.3b). In these tests (Sultan et al., 2002), the samples were initially isotropically loaded to 4 MPa, then heated to 100°C, cooled to 100, 70, 40 and 23°C, and then loaded to over 10MPa.

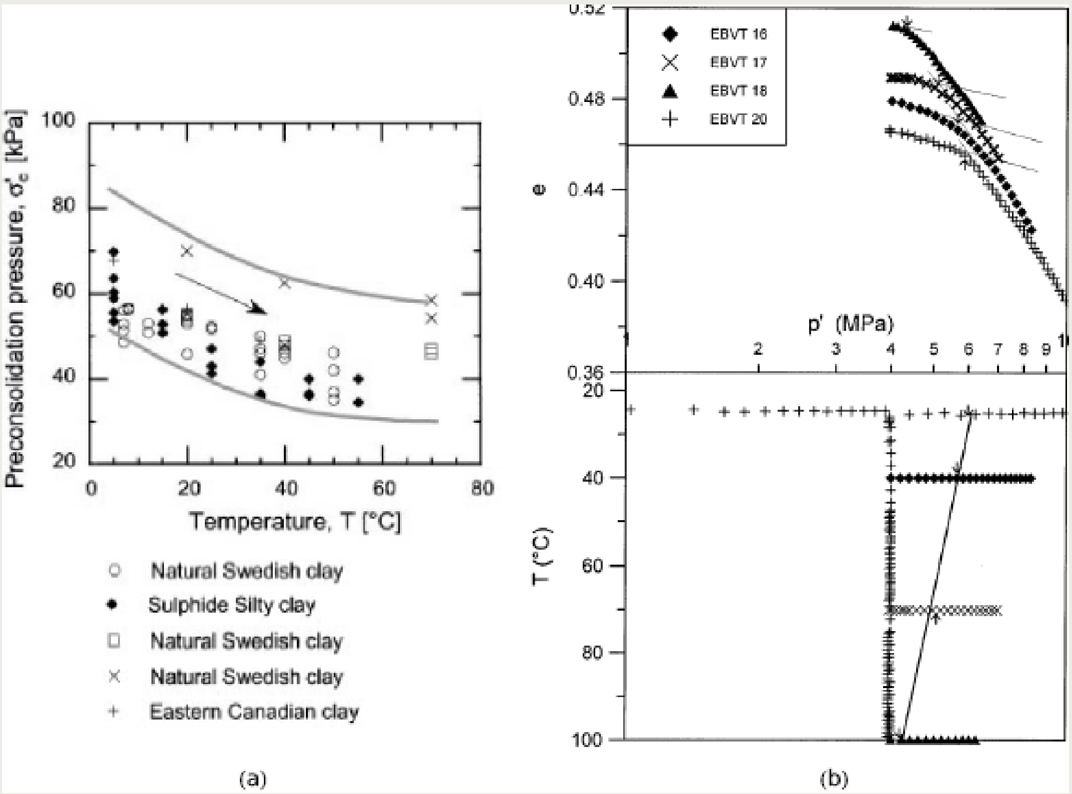

Figure 2.3.: Temperature effects on the pre consolidation pressure; (a) for five different clays (Cekerevac and Laloui, 2004), and (b) for Boom Clay (Sultan et al., 2002) due to thermal loading.

Plastic yield: shear behaviour

A slight decrease in shear strength with increased temperature for Boom Clay was observed by Hueckel and Baldi (1990), Baldi et al. (1991a,b), Hueckel and Pellegrini (1992) and De De Bruyn and Thimus (1996). Interestingly, the effects of the thermal variation of internal friction depend heavily on the history of heating and loading. In particular, the state of stress at which heating is performed, including the OCR, impacts on the ensuing variation of strength (Hueckel et al., 2009). As discussed in Wiseall et al. (2016), De Bruyn and Thimus (1996) observed a reduction in peak friction angle, but no clear change in the critical state friction angle. The observation for the critical state friction angle were supported by the experiments of Horseman et al. (1993), although in their experiments no significant change in peak friction angle was observed either.

Cui et al. (2000) and Sultan et al. (2002) documented that the effects of temperature on shear strength properties have been found to be strongly dependent on the volume changes which were induced by heating. The results also indicated that the thermal softening related to the decrease of water-clay interactions due to heating can be globally balanced by the volume decrease due to thermal consolidation.

De Bruyn and Labat (2002) state that the temperature levels and durations applied during the ATLAS experiment seemed to have no significant influence on the change in strength of the Boom Clay.

Li et al. (2007) pointed out that the limited data available, as well as their scatter, does not allow for a quantitative conclusion on the relation between shear strength and temperature for Boom Clay.

2.7. Coupled hydro-mechanical response

The proceeding sections dealt with the thermal impact on temperature, hydraulic and mechanical behaviour individually. However, as the temperature causes impact on the hydraulic and mechanical components which are intrinsically linked via effective stress, there is a hydro-mechanical response to changes in temperature.

The thermal expansion coefficient of water is generally about one magnitude larger than that of clay and quartz minerals (e.g. section 2.5.1 and Table 2.1 for Boom Clay, Delage, 2013; Ghabezloo and Sulem, 2009; Sultan et al., 2002). The increase in pore-water pressure due to thermal loading can be characterised by the thermal pressurisation coefficient Λ, although in coupled models it is usually better to explicitly model the expansion and pressurisation of the phases independently. Using a heating pulse test under constant volume on natural Boom Clay, a slightly lower value was obtained on cooling than for heating (Lima et al., 2009), although both were higher than the value obtained by Vardoulakis (2002) based on the results of Sultan (1997). This matches the observations of plasticity occurring during heating of Hueckel and Pelligrini (1992) and François et al. (2009).

This increase in pore pressure will typically reduce the effective stress and will move the stress state towards shear failure. This may in turn increase the plastic (damaged) zone around excavations (see François et al. 2009).

2.8. Conclusions

This chapter has presented a brief targeted review of the thermal impact on the THM behaviour of Boom Clay. While data is limited a number of observations can be made. The thermal expansion of the solid and liquid phases is significantly different, yielding pore pressure increases, where water cannot drain. These increases can reduce the mean effective stress and lead to shear failure. Increases in temperature are also observed to increase the hydraulic conductivity (via viscosity reduction) and decrease the pre-consolidation pressure. The shear failure locus is seen to not be significantly affected.

Table 2.1.: Thermal soil property of Boom Clay (after Arnold et al., 2015)

Definition	Symb.	Unit	Value	Depth	Location	Note	Source
Thermal conductivity	λ	W m^{-1} K^{-1}	1.690				Boisson (2005)
			1.350		Mol (B)	Atlas	Li et al. (2007)
			1.700			SAFIR 2	Li et al. (2007)
			1.440		Mol (B)	Lab	Li et al. (2007)
			1.350			Used in analysis	Chen et al. (2011)
			1.450		Mol (B)	Used in isotropic analysis	Weetjens (2009)
			1.350		Mol (B)	Proposed reference equivalent thermal conductivity	Garitte et al. (2012)
			1.350		Mol (B)	ATLAS (standard deviation 0.05)	Garitte et al. (2012)
			1.440		Mol (B)	Lab	Garitte et al. (2012)
			1.690				Horseman and McEwen (1996)
Vertical thermal conductivity	λ_v	W m^{-1} K^{-1}	1.310			Used in analysis	Chen et al. (2011)
			1.250	223.00	Mol (B)	From ATLAS III with reference to report to be published	Weetjens (2009)
			1.060	223.00	Mol (B)	Proposed reference horizontal thermal conductivity	Garitte et al. (2012)
			1.060	223.00	Mol (B)	ATLAS	Garitte et al. (2012)
			1.180	223.00	Mol (B)	Lab	Garitte et al. (2012)
Horizontal thermal conductivity	λ_h	W m^{-1} K^{-1}	1.650			Used in analysis	Chen et al. (2011)
			1.700	223.00	Mol (B)	From ATLAS III with reference to report to be published	Weetjens (2009)
			1.550	223.00	Mol (B)	Proposed reference horizontal thermal conductivity	Garitte et al. (2012)
			1.550	223.00	Mol (B)	ATLAS	Garitte et al. (2012)
			1.600	223.00	Mol (B)	Lab	Garitte et al. (2012)
Degree of anisotropy	λ_h/λ_v	–	1.260				Chen et al. (2011)
			1.360				Weetjens (2009)
			1.462	223.00	Mol (B)		Garitte et al. (2012)
			1.462	223.00	Mol (B)		Garitte et al. (2012)
			1.356	223.00	Mol (B)		Garitte et al. (2012)
Thermal diffusivity	α	m^2 s^{-1}	5.90E-07				Boisson (2005)
			5.96E-07				Horseman and McEwen (1996)
Vol. heat capacity	c	J m^{-3} K^{-1}	2.84E-006				Li et al. (2007)
			2.83E-006				Horseman and McEwen (1996)
Linear thermal dilation coefficient	α_s	m^3 m^{-3} K^{-1}	1.00E-05 – 5.00E-05				Li et al. (2007)
			1.00E-05				Picard (1994)
			1.00E-05			Approximation	Bolzon and Schrefler (2005)
			1.00E-05			Quoted as volumetric in original reference	Vardoulakis (2002)
			4.30E-06			Value taken from François et al. (2009), quoted as volumetric in original reference	Laloui (1993)
			1.67E-05	223.00	Mol (B)	Quoted as volumetric in original reference	Baldi et al. (1987, 1991a,b)
			4.20E-05			Effective stress as 223.00m at Mol, quoted as volumetric in original reference	Monfared et al. (2012)

3. Numerical model

3.1. Introduction

The set-up of the numerical model to simulate the post-operation THM behaviour is presented. The numerical modelling has been undertaken using the commercial software PLAXIS (Plaxis, 2015). This follows from the initial thermal modelling and the mechanical modelling presented in Arnold et al. (2015).

Initially the governing equations are presented and parameterised using information available from chapter 2. Then the domain, boundary conditions and model strategy are presented.

3.2. Modelling strategy

To initially understand the THM behaviour and the potential effects on the Boom Clay, a numerical modelling investigation has been undertaken. A 2D model is considered, due to the disposal tunnels being long compared to their diameter, and the basis of the models was the 2D models presented in Chapter 6 of Arnold et al. (2015). An additional phase has been added to these analyses to include the post-operation behaviour.

The following tasks have been undertaken:

- A thermal parameters analysis – utilising the most likely hydraulic and mechanical properties. Three models are presented based on three different thermal properties: a most likely scenario, as well as high and low range scenarios.

- A mechanical parameter sensitivity analysis – utilising the most likely thermal properties and varying individual important model parameters, to assess their impact on the extent of the plastic zone and the liner forces.

3.3. Governing Equations

These equations are summarised from Plaxis (2015) and Galavi (2010) and simplified for saturated conditions as found in this situation.

3.3.1. Thermal behaviour

The heat energy balance equation for the porous medium can be written as (see equation 2.1):

$$\frac{\partial T}{\partial t}(C\rho) = -\nabla.(J_{Tw} + J_c) + Q_T \tag{3-1}$$

where J_{Tw} and J_c are the advective heat flux in water and conductive heat flux, respectively. The conductive heat flow is assumed to be governed by Fourier's law:

$$J_C = -\lambda\nabla T \tag{3-2}$$

where the thermal conductivity can be defined as a mixture:

$$\lambda = (1-n)\lambda_s + n\lambda_w \tag{3-3}$$

where n is the porosity, λ_s is the solid thermal conductivity and λ_w is the water thermal conductivity. The advective internal energy flux in water is:

$$J_w = \rho_w C_w T V_w \tag{3-4}$$

where V_w is the velocity of the water phase and C_w is the specific heat capacity of the water. In Boom Clay the water velocity is low and this term does not play a significant role in the heat transport.

The volumetric heat capacity can be defined as a mixture:

$$C\rho = (1-n)\rho_s C_s + n\rho_w C_w \tag{3-5}$$

where C_s and C_w are the solid and water specific heat capacities.

3.3.2. Hydraulic behaviour

The mass balance equation for flow in a porous medium can be written as:

$$\frac{\partial n\rho_w}{\partial t} = -\nabla.(J_w) \tag{3-6}$$

where J_w is the advective flux of water, which can be defined via Darcy's law as:

$$J_w = -\frac{K}{g\rho_w}(\nabla p_w + \rho_w g) \tag{3-7}$$

The first term of equation 3-6 can be written as:

$$\frac{\partial n\rho_w}{\partial t} = n\frac{\partial \rho_w}{\partial t} + \rho_w\frac{\partial n}{\partial t} \tag{3-8}$$

and re-written including the compressibility of water as:

$$\frac{\partial n\rho_w}{\partial t} = n\rho_w\beta_{wP}\frac{\partial p_w}{\partial t} + \rho_w\frac{\partial n}{\partial t} \tag{3-9}$$

The second term (on the right hand side) can be determined from the coupling with the mechanical equation and the final equation yields:

$$n\rho_w\beta_{wP}\frac{\partial p_w}{\partial t} + \rho_w\frac{\partial n}{\partial t} = \nabla\left[\frac{K}{g\rho_w}(\nabla p_w + \rho_w g)\right] \tag{3-10}$$

3.3.3. Mechanical behaviour

The mechanical behaviour is defined by the momentum balance, which, for the porous medium, can be given by:

$$\nabla.\boldsymbol{\sigma} + \rho\mathbf{g} = 0 \tag{3-11}$$

where $\boldsymbol{\sigma}$ is the total stress tensor, $\mathbf{g}$ is the gravitational matrix (where the entry associated with vertical stresses is filled with the gravitational constant) and the density can be defined as a mixture by:

$$\rho = (1-n)\rho_s + n\rho_w \tag{3-12}$$

The principle of effective stress is used, such that:

$$\boldsymbol{\sigma} = \boldsymbol{\sigma}' + p_w\mathbf{m} \tag{3-13}$$

where $\boldsymbol{\sigma}$' is the effective stress tensor and $\mathbf{m}$ is the identity tensor.

The constitutive behaviour is defined incrementally as:

$$d\boldsymbol{\sigma}' = \mathbf{M}(d\boldsymbol{\varepsilon} - d\boldsymbol{\varepsilon}_T^e) \tag{3-14}$$

where $\mathbf{M}$ is the material matrix which includes the elastic and plastic behaviour, $d\boldsymbol{\varepsilon}$ is the incremental strain and $d\boldsymbol{\varepsilon}_T^e$ is the incremental (elastic) thermal strain, which follows equation 2-6.

The constitutive behaviour is defined using the Hardening Soil model from PLAXIS, following the previous calibration of parameters for Boom Clay by Arnold et al. (2015).

3.4. Model set-up

3.4.1. Analysis stages

The analysis was conducted in 3 stages:

i. a K0 stage (shown in Fig 3.1a), where the initial vertical and horizontal stresses were calculated;

ii. an excavation and construction stage, where the tunnel lining was included and then contracted to represent the relaxation of the Boom Clay into the overcut (see Arnold et al., 2015 for more details); and

iii. a heating THM stage, where a heat flux representing the flux from the emplaced waste was applied to the tunnel boundary.

3.4.2. Domain

The model domain is shown in Fig. 3.1. The main calculation domain (Fig. 3.1b and c) was 25 × 160m, discretised using 15-node triangular elements and refined throughout due to the expected THM processes occurring throughout the domain. The domain was chosen to be 25 m wide due to symmetry of the system, with the tunnel at the left boundary and the mid-point between the adjacent tunnels on the right.

The initial vertical effective stress in the domain was set to increase with depth (10 kPa/m,) with a total vertical stress of 4.2 MPa being applied along the top boundary and the pore pressure being initially hydrostatic (see Arnold et al. 2015). The initial temperature set to 295 K, which corresponds to the value found experimentally at 500m depth in Belgium by Vandenberghe and Fock (1989). The bottom mechanical boundary was fixed, whereas the left- and right-side boundaries were fixed in the horizontal direction (due to symmetry) and free in the vertical direction. The temperatures were fixed at 295 K (the initial condition) at the top and bottom of the domain, and the left- and right-side boundaries were set to a zero heat flux due to symmetry. Similarly, the left- and right-side boundaries were set to a zero porewater flux. The base boundary was impermeable and the top boundary was a fixed pore pressure.

A time-dependent boundary condition has been set on the tunnel outer boundary to represent the heat generation from the waste. An initial heat flux of 12.5 W/m^2 was applied and reduced over time, based on the expected radioactive decay. This decay was presented in Arnold et al. (2015) and is shown in Figure 3.2. A further discussion on the appropriateness of this boundary condition is given in Section 4.5.

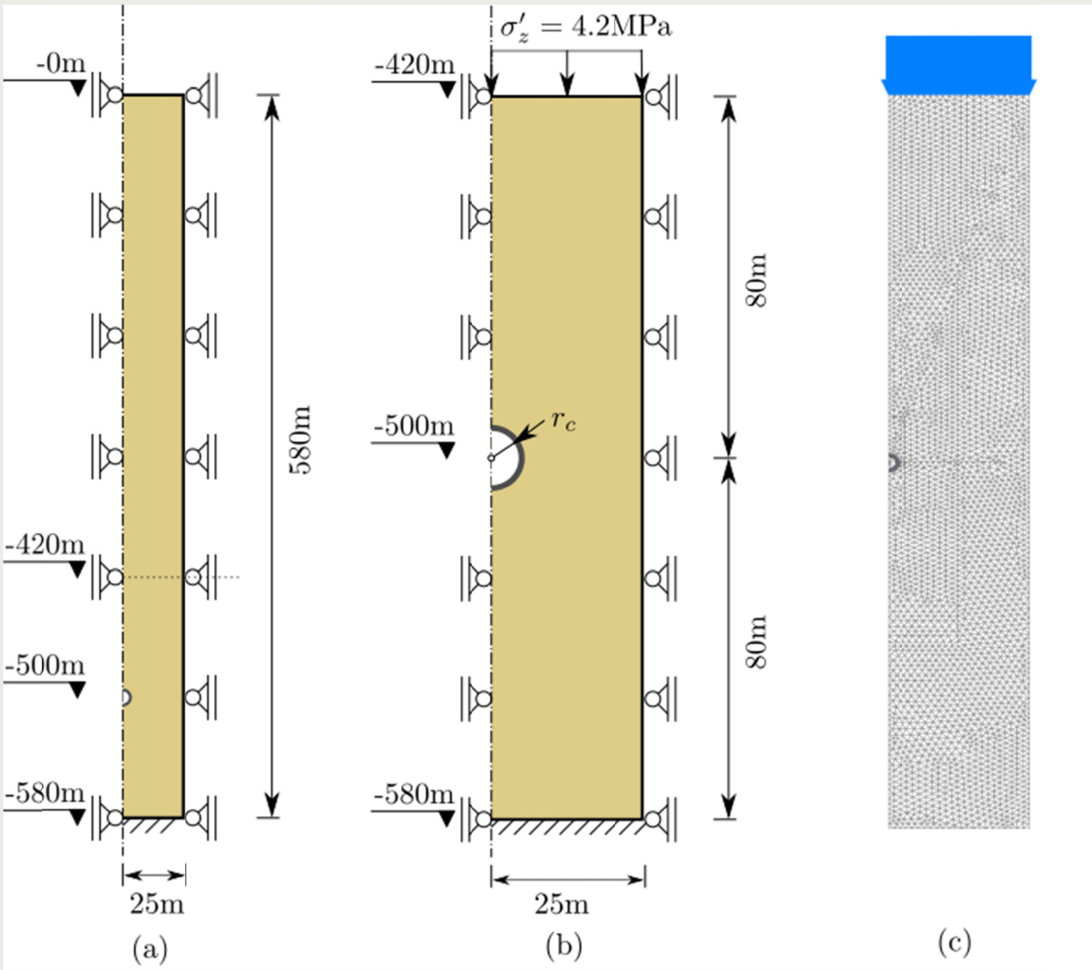

Figure 3.1.: Model details, (a) preliminary model domain for the K0 procedure, (b) the calculation domain and (c) the mesh for the excavation and THM stages.

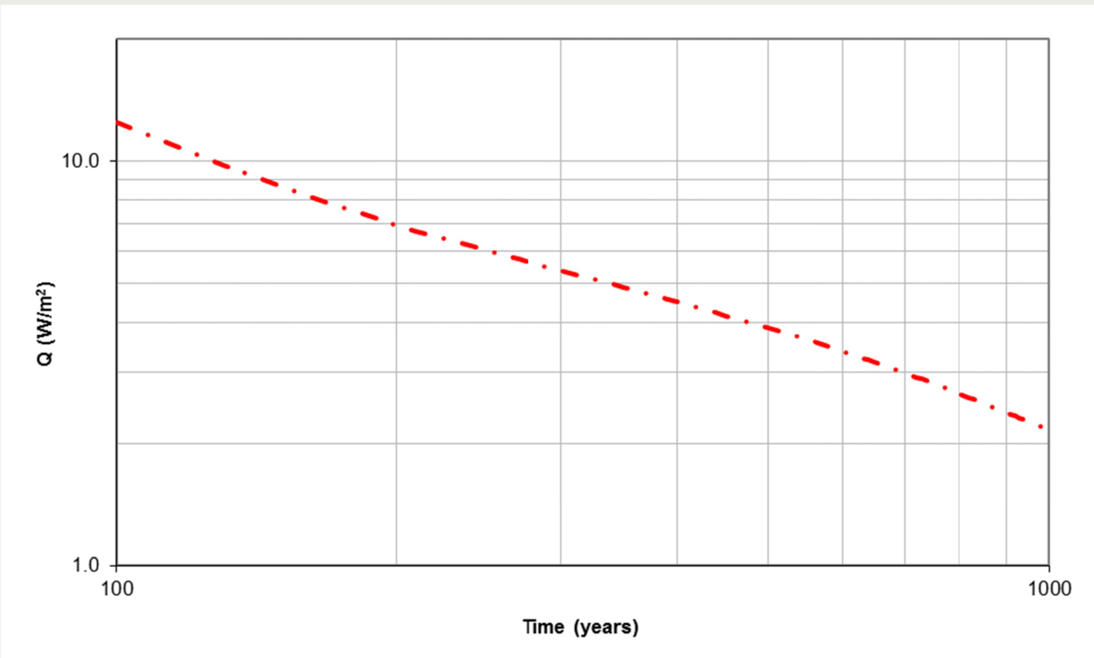

Figure 3.2.: The applied heat flux on the tunnel external boundary.

3.4.3. Thermal scenarios

Three sets of thermal properties were considered: Scenario High refers to the highest calculated temperatures in the Boom Clay, assuming the lowest value of the Boom Clay thermal conductivity; Scenario Low refers to the lowest calculated temperatures in the Boom Clay; and Scenario Mid refers to a scenario mid-way between the two, and can be considered the most likely. This allows an indication of the sensitivity of the thermal behaviour to main heat transfer properties of the Boom Clay. The material parameters that form these scenarios are found in Table 3.1a and are the same as those presented for the thermal analysis in Arnold et al. (2015).

These have been decomposed for the computational analysis into solid components, so that the mixture equation presented in section 3.3 can be used. These are based on the values in Table 3.1b, using the values of pure water (Kaye and Laby, 1973), a void ratio of 0.7, a solid density of 2600 kg m^{-3} (e.g. Mitchell and Soga, 2005), and a solid specific heat capacity of clay solid of 800 J kg^{-1} K^{-1} (e.g. Börgesson and Hernelind, 1999):

Table 3.1a.: Parameters for thermal analyses for different scenarios for bulk material.

Parameter	Symb.	Unit	Scenario High	Scenario Mid	Scenario Low
Bulk density (sat)	ρ	kg m^{-3}	1900	2000	2100
Thermal conductivity	λ	W m^{-1} K^{-1}	1.06	1.4	1.7
Specific heat capacity	C	J kg^{-1} K^{-1}	1333	1400	1470

Table 3.1b.: Parameters for thermal analyses for different scenarios for solid material.

Parameter	Symb.	Unit	Scenario High	Scenario Mid	Scenario Low
Solid density	ρ_s	kg m^{-3}	2600	2600	2600
Solid thermal conductivity	λ_s	W m^{-1} K^{-1}	1.405	2.000	2.525
Solid specific heat capacity	C_s	J kg^{-1} K^{-1}	800	800	800

3.4.4. Material parameters

The base material properties are based on the most likely parameters found by Arnold et al. (2015). The mechanical parameters are presented in Table 3.2, the hydraulic parameters in Table 3.3 and the additional thermal parameters in Table 3.4. The hydraulic conductivity has been selected as isotropic, with a value that is approximately the mean of the values found in literature (see Appendix A2, Arnold et al., 2015). Note that this is an assumption, to allow scoping of the response. Detailed analysis of the anisotropy of the impact of hydraulic conductivity will be needed in the future. The additional thermal property is only the thermal expansion coefficient of the solid, which is selected based on Table 2.1 at 0.33×10^{-5} K^{-1}. It is clear from literature that there is some uncertainty in this parameter and it has therefore been varied in the sensitivity analysis chapter, along with other key parameters.

In this model, it is not yet possible to include plastic yield functions and thermal dilation coefficients as temperature dependent, which is a limitation of this work. The change of hydraulic conductivity with deformation has not been used due to a lack of information, but automatically updates for temperature driven changes in water viscosity.

Table 3.2.: Mechanical parameters

Parameter	Symb.	Unit	Value
Shear strength			
Effective friction angle	ϕ	°	12.5
Effective cohesion	c	MPa	0.5
Dilatancy angle	ψ	°	0
Stiffness			
Reference secant modulus	E_{50}^{ref}	MPa	145
Reference un/reloading modulus	E_{ur}^{ref}	MPa	435
Reference oedometer modulus	E_{oed}^{ref}	MPa	145
Rate of stress dependency of stiffness	m		0.7
Un/reloading Poisson's ratio	ν_{ur}	-	0.3
Other			
Reference stress	p^{ref}	MPa	0.1
At rest earth pressure	K_0	-	1.0
OCR	OCR	-	2.2
Failure ratio	R_f	-	0.9

Table 3.3.: Hydraulic parameters

Parameter	Symb.	Unit	Value
Hydraulic conductivity	K	$m\ s^{-1}$	4×10^{-12}
Initial void ratio	e_0	-	0.7

Table 3.4.: Thermal parameters

Parameter	Symb.	Unit	Value
Linear thermal expansion coeff.	α_s	K^{-1}	0.33×10^{-5}
(Volumetric thermal expansion coeff.	β_{Vs}	K^{-1}	1.00×10^{-5})

4. Results

4.1. Introduction

The results from the three thermal scenarios are presented in this section. The temperature and pore pressure distributions are discussed along with the stress behaviour. In Figure 4.1 the thermal results, expressed as temperature contour plots, are presented, with complimentary plots presented in Figure 4.4. In Figure 4.2 the pore pressure results are presented, also with complimentary plots in Figure 4.4. In Figure 4.3 the mechanical results in terms of the plastic zone are presented with a more detailed analysis of the stresses and resulting liner moments in Figures 4.5 to 4.8. The results presented here focus on the period between emplacement and 127 years. This is when the maximum temperature, pore pressure and plastic behaviour of the Boom Clay were found to occur.

4.2. Scenario Mid

In the mid case scenario, as seen in Figure 4.4(c) the maximum temperature of 335 K (62°C) is reached at the tunnel edge after 127 years of heating from 295 K. After that, the temperature at the container surface decreases slowly with time. This is in contrast with the report of Arnold et al. (2015), which reported an earlier peak time of between 30 and 60 years. This was due to a step-wise boundary condition used in that work (due to the limitation of the PLAXIS version at that time), whereas now a smooth boundary condition is used. Therefore, more confidence is given in these results. During the time period of 60 – 127 years there is less than a 2°C difference in temperature at the tunnel edge. The temperature at the tunnel edge begins to reduce after this time (not shown in the figure). As expected, the temperatures rise increasingly slowly the further away from the tunnel edge in all directions. Heat can only escape from the domain vertically, due to the zero-flux boundary, representing interaction from adjacent tunnels, which causes the long peak, as opposed to e.g. Weetjens (2009) who uses an axi-symmetric model, neglecting the effect of adjacent tunnels.

The pore pressure can be seen in Figure 4.4(d) to increase, from the in-situ conditions of 5 MPa, rapidly at the tunnel boundary until just over 5.5 MPa, with an decreasing spatial gradient away from the tunnel. This is due to the thermal expansion of both the soil and the water with temperature. After this initial rapid rise, the pore pressure continues to rise, but the spatial gradient is increasingly small, with the pore pressure controlled more by the vertical flow through the Boom Clay, as can be observed by the near vertical gradients in Figure 4.2. The pore pressure reaches a peak of just over 6.3 MPa at 127 years, suggesting that the pore pressure is more controlled by the temperature rise than the ability of the water to escape the system. The pore pressure is significantly below the insitu total stress meaning also that localised damage, i.e. hydraulic fracturing is unlikely.

The plastic zone shown in Figure 4.3 is seen to significantly change shape, from the near uniform circular shape around the tunnel due to tunnel construction, to an almost symmetrical lobed shape comprising vertical plastic lobes and an elastic unloading zone spreading horizontally from the tunnel wall. Two competing thermo-mechanical processes are causing this process. The first is the thermal expansion of the solid material. In isolation this causes the solid material to expand, causing either expansive volumetric strains or an increase in compressive stress. The second is the thermal expansion of the water, which causes an increase in pore pressure or a flow of water. An increase in pore pressure also causes a reduction in the mean effective stress (acting on the solid) and therefore a decrease in compressive stress or an expansion. In the analysed domain, in the horizontal direction the deformation is fixed at the boundary (due to symmetry of the physical system) and the domain of influence is narrower than in the vertical direction. In the vertical direction the boundary is stress controlled. This means that the solid thermal expansion is likely to increase the horizontal stresses and deformation is more likely in the vertical direction, having the effect on changing the deviatoric stress q in the horizontal direction and leaving it almost unchanged in the vertical direction.

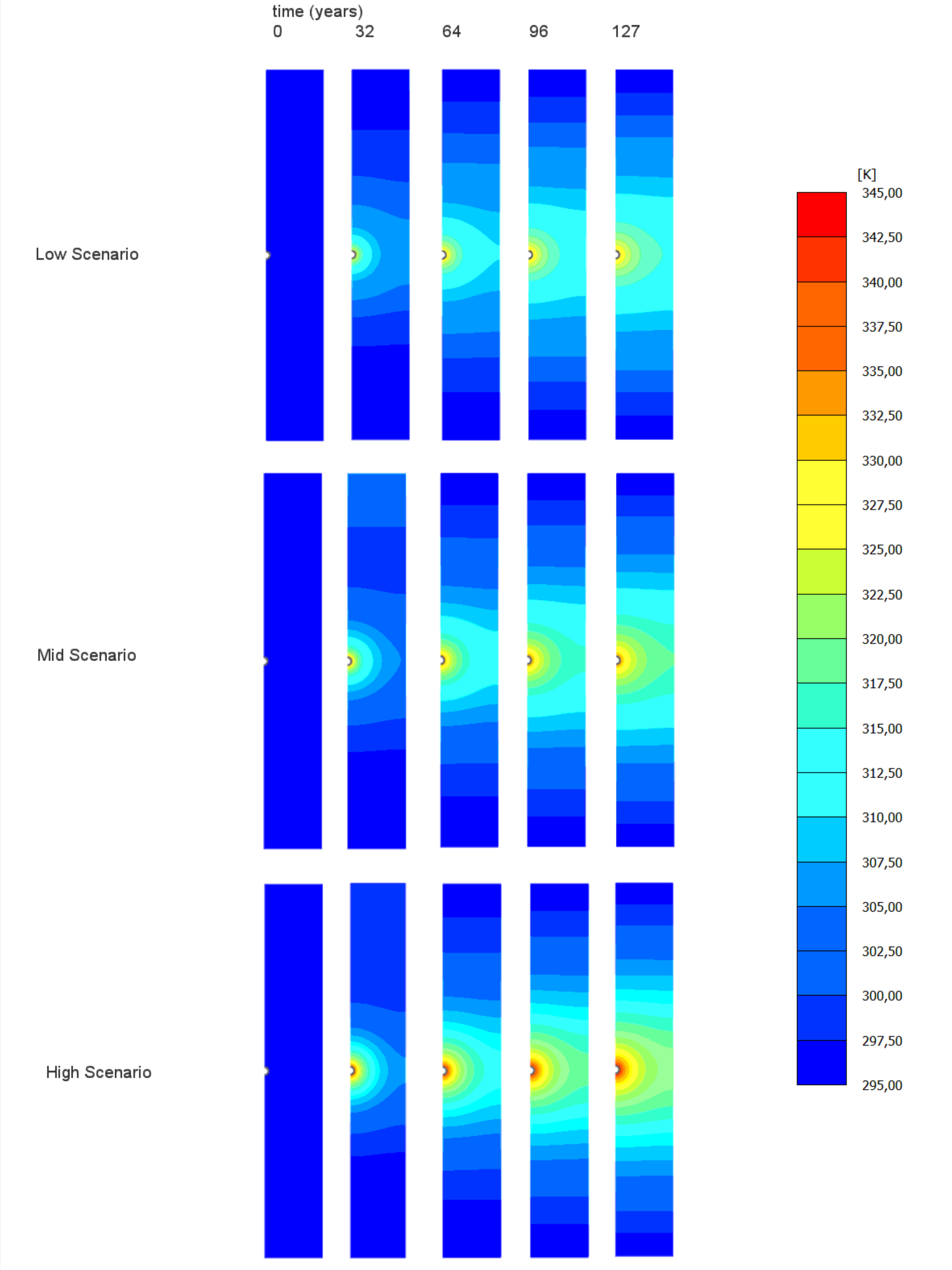

Figure 4.1.: Temperature results from the three thermal scenarios.

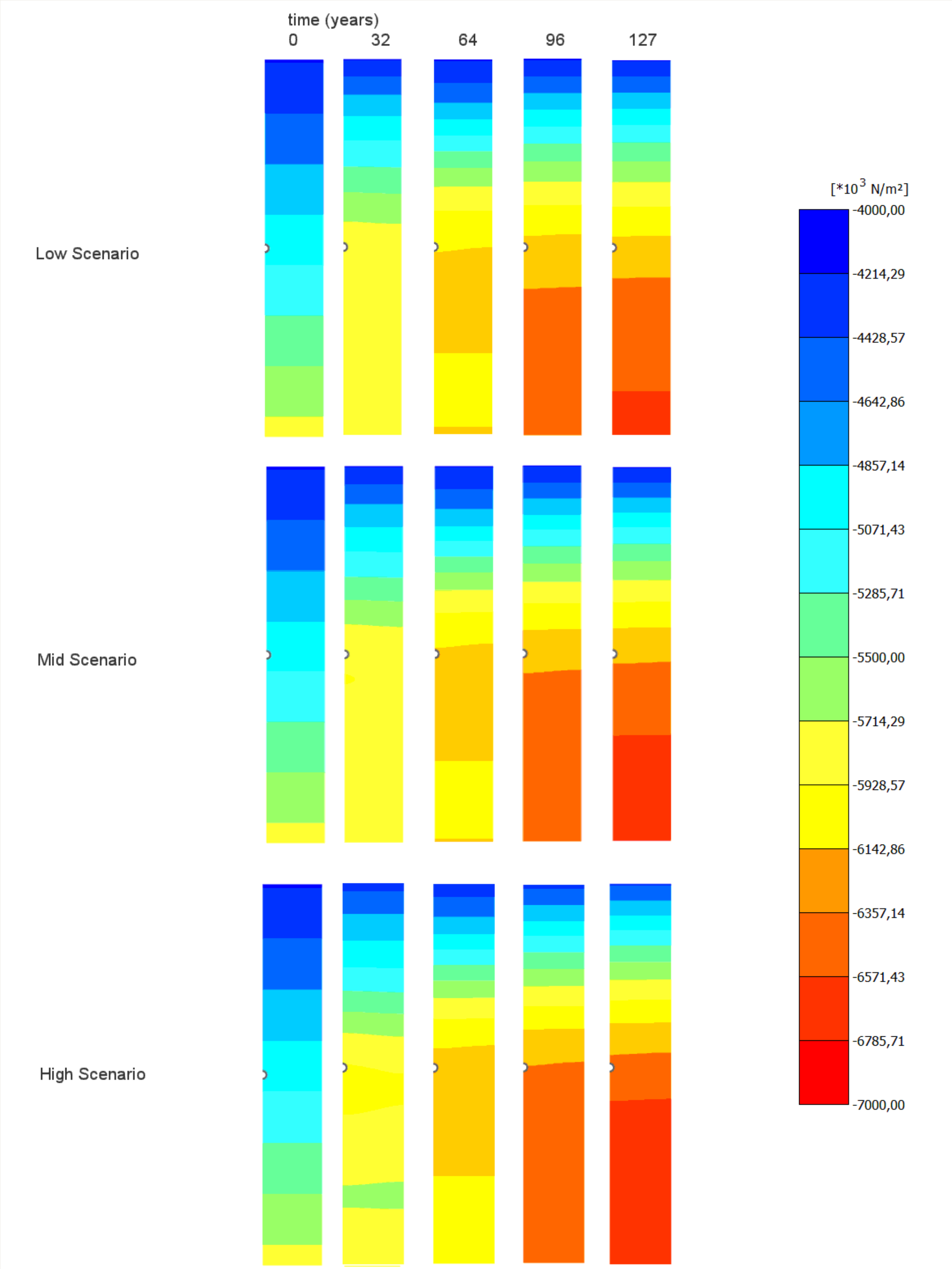

Figure 4.2.: Pore pressure results from the three thermal scenarios.

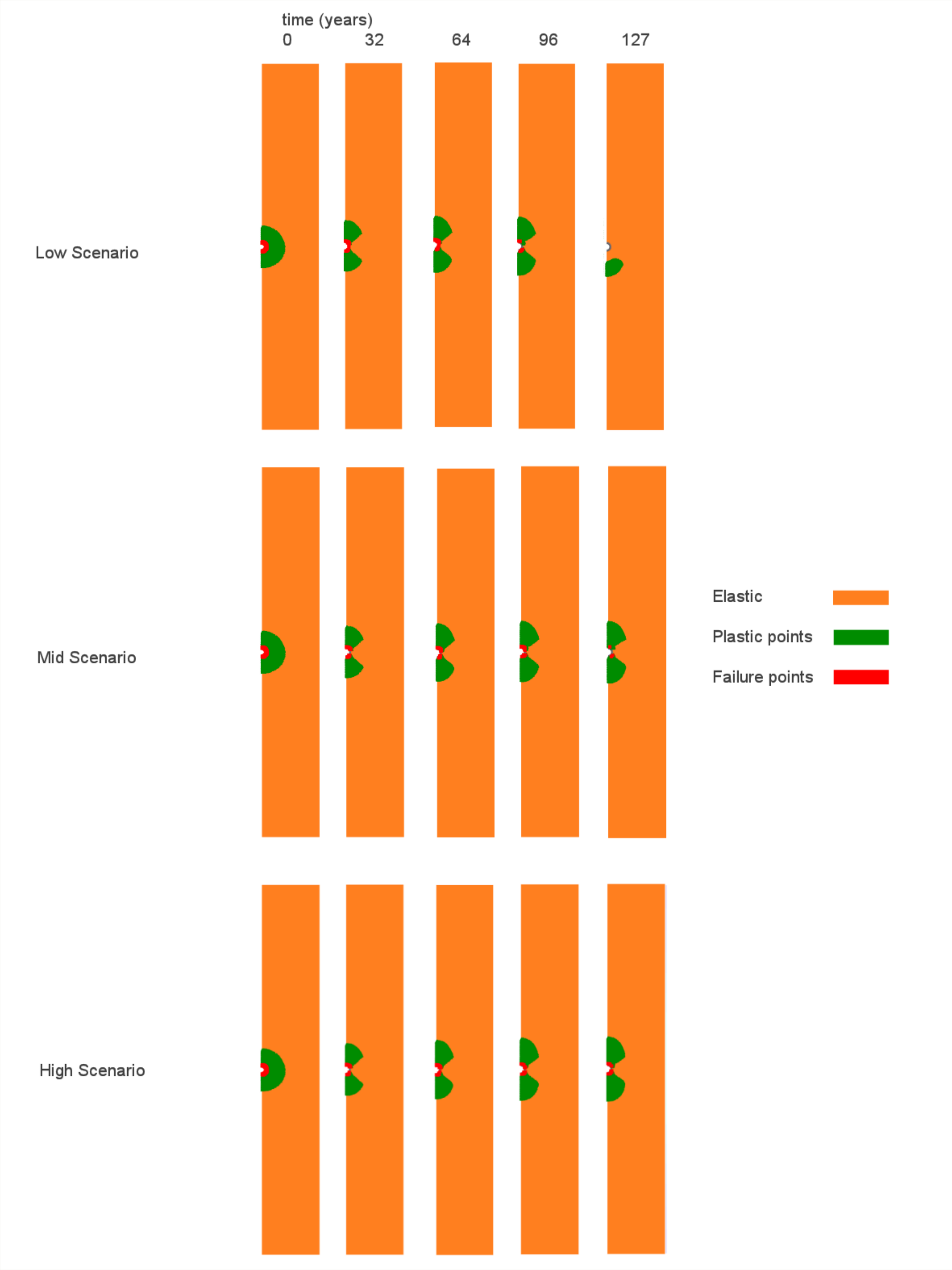

Figure 4.3.: Plastic point results from the three thermal scenarios

In Figure 4.5 the mean effective stress and deviatoric stress (p'-q) are shown along a line radiating horizontally from the tunnel axis. Following the closest point to the tunnel surface (1.73 m from the tunnel centre, shown by black squares) the initial rise in q at near constant p' is elastic unloading (A to B shown on Figure 4.5), due to the tunnel construction. The portion of the stress path curving to the left (increasing q and decreasing p', B to C on Figure 4.5) is due to further unloading to the tunnel construction and plastic deformation. This location then fails when it hits the failure line (the peak q, point C) and follows the failure line as further deformation occurs (point C to D). The end portion of this curve (point D to E) is due to the thermal part of the analysis, where, as the pore pressure increases further plasticity occurs, locally maintaining the effective stress. Further away from the tunnel, at approximately 4, 6 and 11 m, the effective stress reduces due to the increased pore water pressure, however the deviatoric stress also decreases as the Boom Clay is compressed due to the clay trying to expand, resulting in elastic unloading. This is due to the minor principle stress being horizontal close to the tunnel, so that increases in the horizontal stress reduce deviatoric stress. Even further away from the tunnel (>13 m), as the pore pressure rises p' also decreases, but after an initial reduction in q the stress direction reverses (the minor stress becomes vertical) and increases in horizontal stress results in increased shear stress, i.e. q increases. In this case q does not rise enough to cause plasticity, however it is noted that it makes plasticity more likely and, as can be observed in Chapter 5, plasticity caused in this way can cause a plastic zone surrounding the entire heat producing section of the repository. The reduction in p' during the first 127 years can be observed throughout the domain in Figure 4.6(a) and the change in the distribution of q can be seen in Figure 4.6(b). The stress direction change, coinciding with the minor stress moving from horizontal to vertical can be seen in Figure 4.7.

The result of these changes in stress state lead to changes on the liner and therefore implications for the stability of the liner. The maximum stress on the liner increases from 5.8 to 6.8 MPa, which, following the approach in Figure 4.4 of Arnold et al. (2015), is not significant for concrete with a compressive strength of either 45 or 80 MPa and the proposed 0.5 m thickness. In fact, a reduction in thickness, as suggested by Arnold et al. (2015) may be possible. Of more significance is the change in the moment predicted on the lining, due to the vertical and horizontal differences. This increases from ~60 kNm/m to ~110 kNm/m. The detailed design of the tunnel lining is beyond the scope of this work, although the moment resulting from the thermal period should be included.

4.3. Scenario High

In the high scenario the thermo-hydro-mechanical behaviour is similar, with an increased maximum temperature of 343K (70°C) and a maximum pore pressure of 6.4 MPa. The increased pore pressure results in a slightly increased plastic zone (Figure 4.3), although the overall shape and behaviour are similar. The maximum stress on the lining increased to 6.9 MPa, mainly due to the increased pore pressure, and the moment has increased to 120 kNm/m.

4.4. Scenario Low

In the low scenario the thermo-hydro-mechanical behaviour is similar, with a decreased maximum temperature of 330K (57°C) and a maximum pore pressure of 6.2 MPa. Moreover, the pore pressure has peaked and started to reduce by around 110 years, leading to an unloading of the system which results in a large reduction of the plastic zone (see Figure 4.3). This does not mean that this zone is undisturbed, and it has still been damaged, but it is not currently yielding. This is due to the thermal consolidation, i.e. compression of the system. The maximum stress on the lining has reduced to 6.7 MPa and the moment to 105 kNm/m.

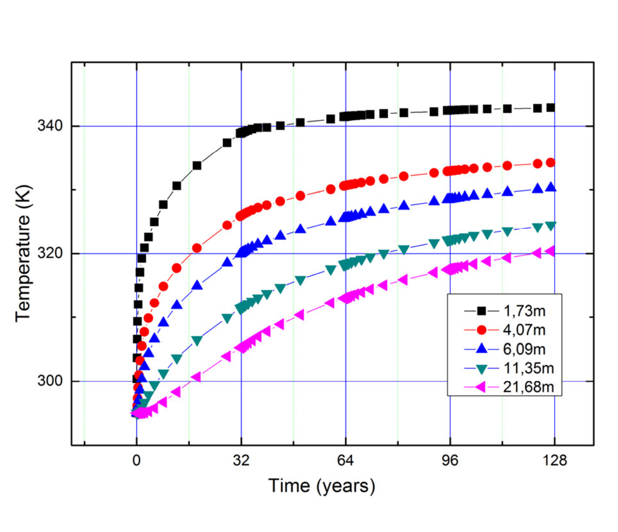

(a) temperature – high scenario

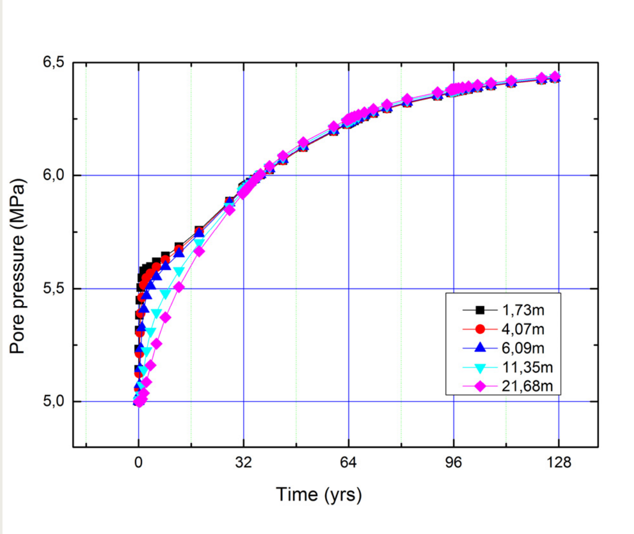

(b) pore pressure – high scenario

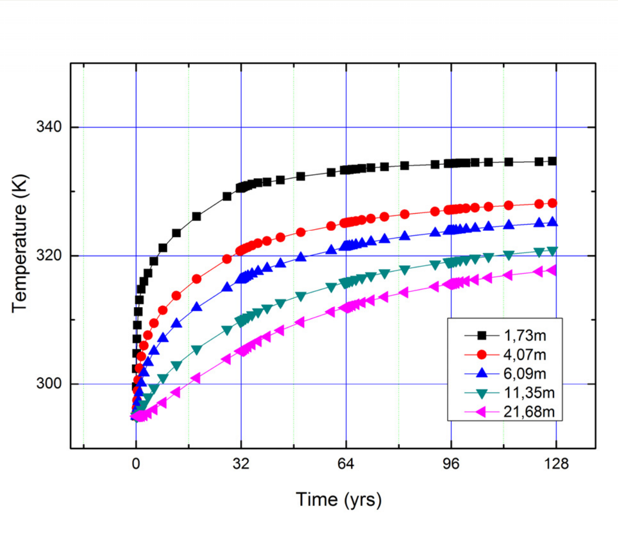

(c) temperature – mid scenario

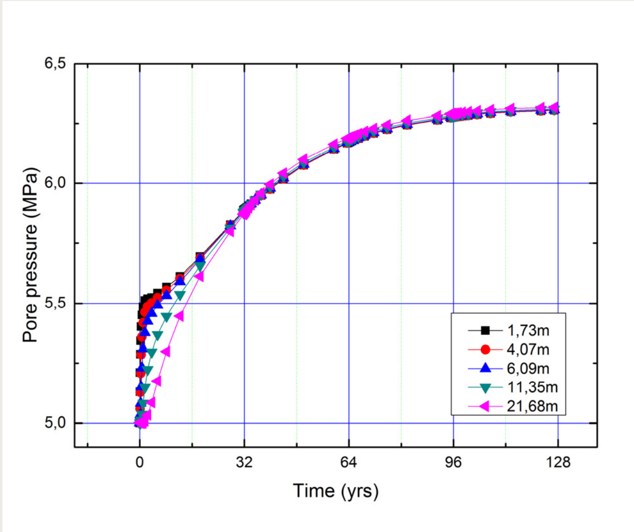

(d) pore pressure – mid scenario

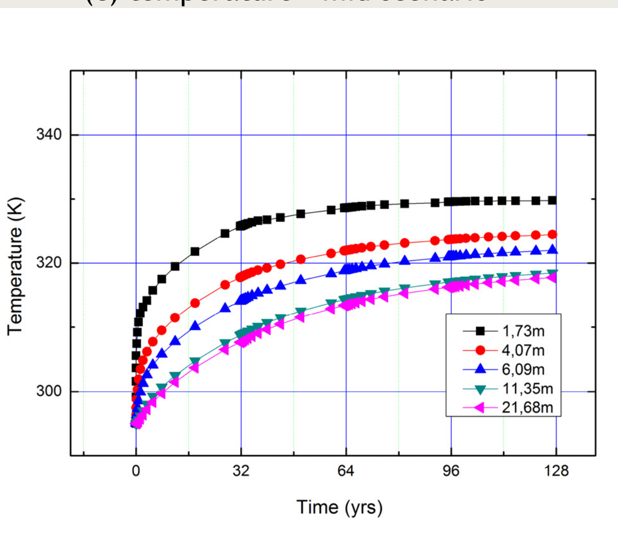

(e) temperature – low scenario

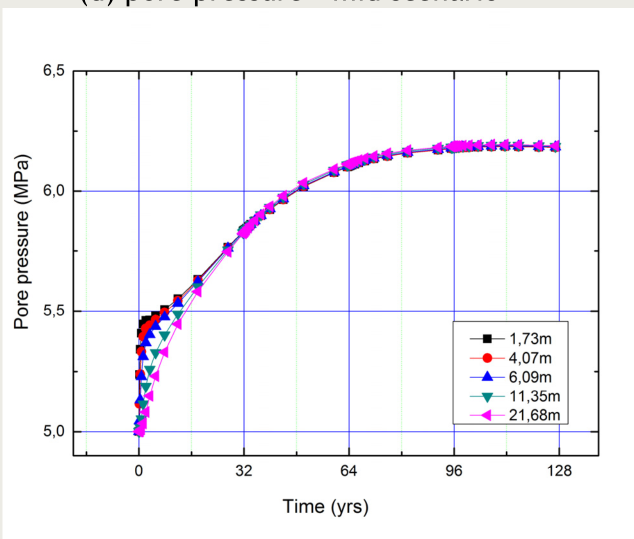

(f) pore pressure – low scenario

Figure 4.4.: Temperature and pore pressure evolution for the high, mid and low scenarios (distances are horizontal and relative to the tunnel axis)

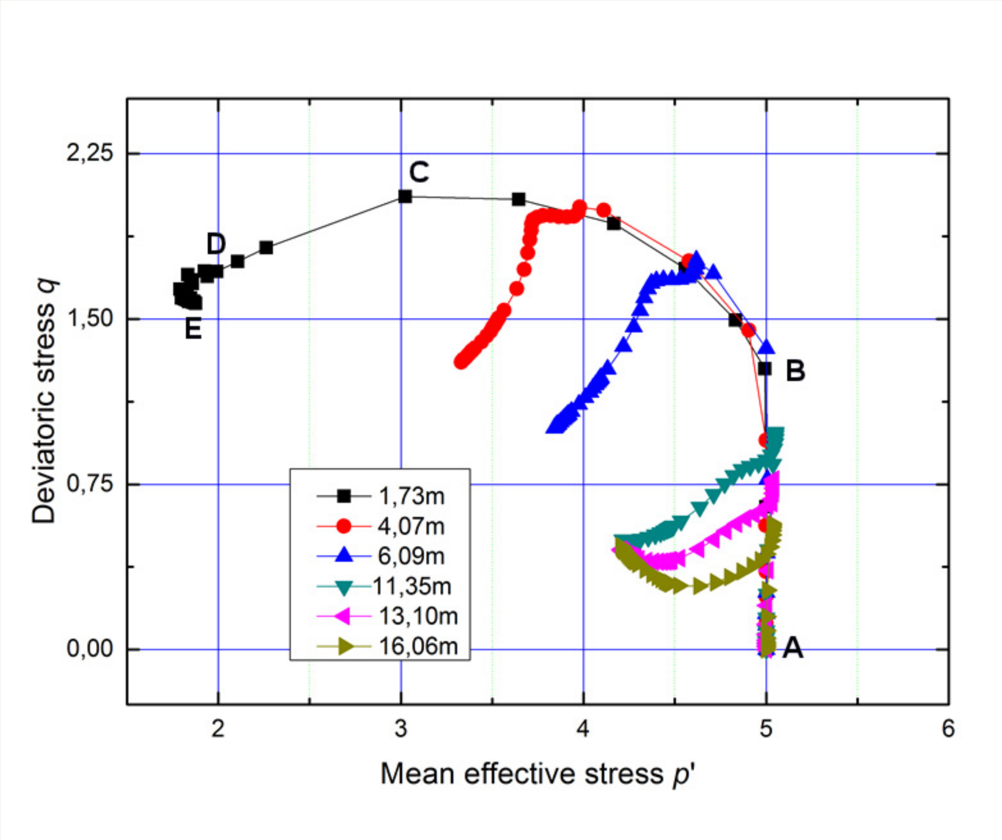

Figure 4.5.: p' and q stress paths (mid scenario); distances are horizontal and relative to the tunnel axis.

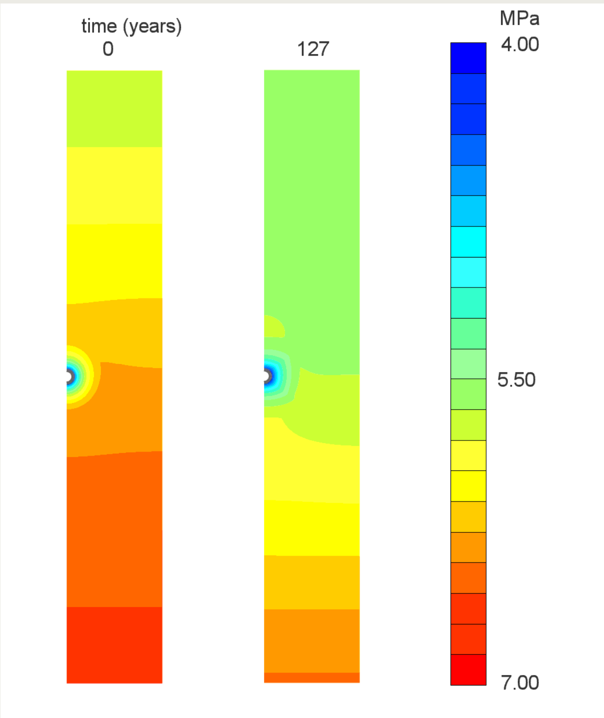

(a) mean effective stress, p'

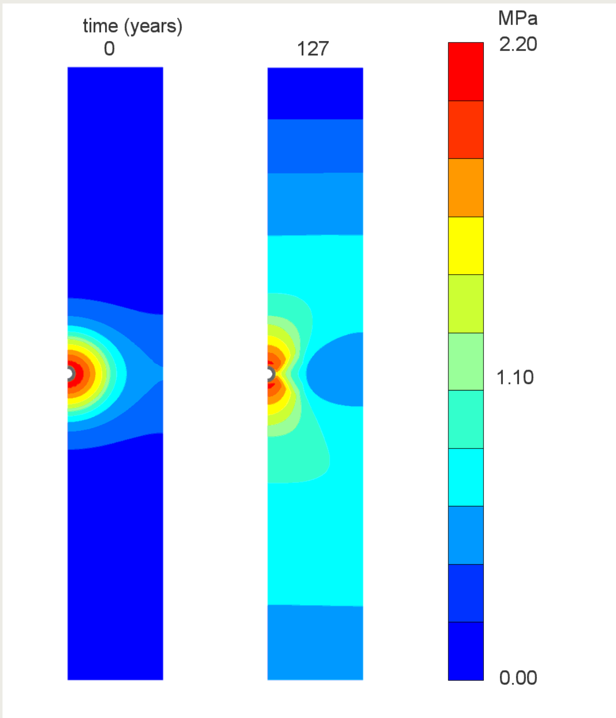

(b) deviatoric stress, q

Figure 4.6.: p' and q contour plots (mid scenario)

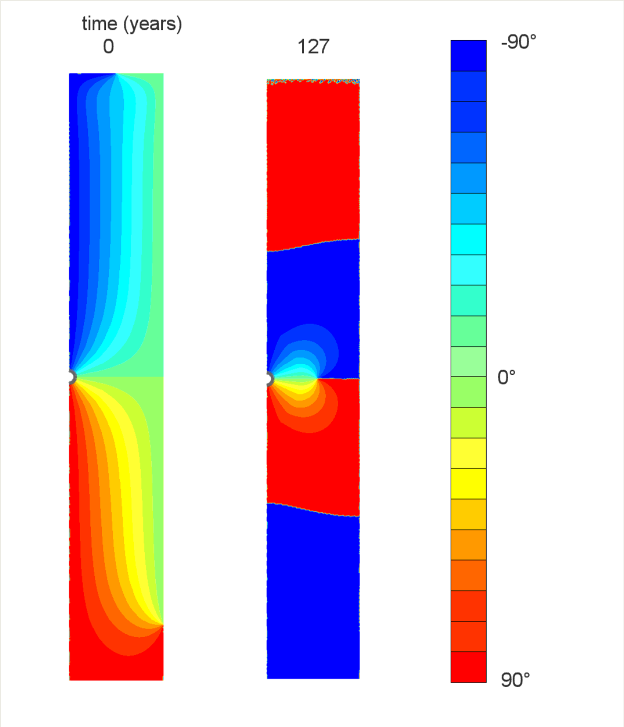

Figure 4.7.: Principle effective stress directions (0° is the major principle stress in the vertical direction).

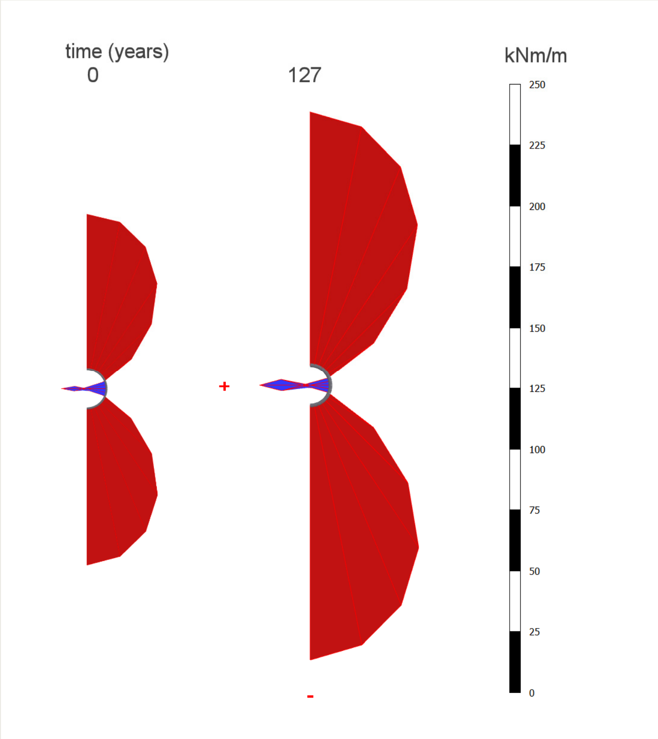

Figure 4.8.: Moments on the tunnel lining

4.5. Discussion

Thermal

As was seen in Arnold et al. (2015), for each scenario the temperature rise is greatest closest to the tunnel, which peaks in temperature after around 100 years (although is steady after about 60 years) and is maintained for a considerable time, due to the interaction between the tunnels. It is noted that the temperature behaviour calculated here is distinctly different than that calculated by Weetjens (2009), where an axi-symmetric model is utilised and the interaction between tunnels is neglected (see Figure 8.4 of Arnold et al., 2015 for further comparison of these approaches). Moreover, with an increased period of surface storage, the heat flux is lower, resulting in a lower temperature increase, with a later peak and less steep rate of decrease afterwards. The temperature further away from the tunnel continues to rise as the temperature pulse moves through the domain. As expected, the smaller the thermal diffusivity the higher the peak temperature. As was also found in Arnold et al. (2015), no scenario considered here yields a peak temperature in excess of limits considered elsewhere, and all peak temperatures are below those where it is considered possible that the minerology of the clay could be changed.

Hydraulic

The pore pressure generation is almost equal in each of the thermal scenarios. This is due to the (near) linear thermal expansion of water and the (near) incompressibility of water, which means that the water can transfer pressure relatively easily throughout the domain, especially in the horizontal direction where the domain size is significantly smaller. The total amount of heat that has entered each simulation is equal, and therefore the total increase in pore pressure is almost the same. Consequentially, it can be seen that the area where the porewater pressure is elevated is greater than that of the temperature. However, in the scenarios with lower temperatures (higher thermal diffusivity), some heat has left the domain and this results in lower pore pressures. While not significant in terms of absolute pore pressures, these pore pressures reduce the effective stress, increase the size of the plastic zone and increase the stresses (and moments) on the liner.

As the temperature increases, it is seen that the pressure gradient in the domain is almost vertical. The means that there is the potential for flow away from the repository. While relatively little water movement over the entire domain would reduce the pressure gradient, if preferential pathways exist a more substantial advective movement of water could occur. This hydraulic gradient will reverse when temperatures fall significantly (as the water will shrink).

Mechanical

As demonstrated by the analyses in this section, the pore pressure generation and the thermal expansion of the solid material cause a considerable change in the plastic zone around the tunnels. Unloading occurs around the tunnel horizontally and the vertical extent of the plastic zone increases. In this zone around the repository the permeability will increase, due to both unloading and damage, i.e. plasticity. While it was shown in the literature (section 2.5.2) that the temperature itself would have little effect on the permeability, there was no information on the change due to damage, i.e. shear failure. The known sealing behaviour of Boom Clay may reduce this impact, but it is thought that this should be experimentally determined.

After the temperature and pore pressures peak, unloading occurs and due to consolidation the material is likely to be denser, stiffer and stronger. This implies that after the thermal period, the Boom Clay properties may have mechanically improved.

In the models shown here, due to limitations of the adopted software and material model, there is no influence of temperature on the yield surfaces. The impact of raising the temperature is that the yield surfaces would reduce and the plastic zones would therefore increase. The quantitative impact should be further investigated both experimentally on representative Boom Clay (as also recommended by Wiseall et al., 2016) and numerically on the repository system.

The impact of the increase in temperature on the tunnel stability in these scenarios seems to be limited. A moderate increase in both the maximum cavity pressure and moment is observed, and should be taken into account in the detailed design of the liner, but neither are sufficiently large to suggest that the construction is not feasible. Additionally, these additional stresses and moments only occur after repository closure, and therefore may affect the ability to retrieve the waste, but would not affect the operational phase of the repository.

A number of longer term mechanical features are not included in the material model used here. These include creep and sealing behaviour. Both processes are likely to aid the sealing of any zones of increased permeability, and creep may lead to an increased maximum stress on the tunnel. For a complete mechanical understanding these processes could be included in future analysis.

Heat output

All of the models utilise the heat output calculated in Arnold et al. (2015), . It is noted in that report that, while this output is based on spent fuel (UOX) and calculated based on a generation II reactor, the majority of the spent fuel comes from research reactors and therefore will have a lower thermal output. The heat output calculated at time of emplacement is supported via the waste inventory reported by Meeussen and Rosca-Bocancea (2014) and Verhoef et al. (2016), although the evolution of the heat output, i.e. the reduction of heat output in time, has been assumed based upon the method of Sillen and Marivoet (2007). This heat output evolution should be further investigated to produce more accurate results. Moreover, this heat output (per metre length of tunnel) can be to some extent controlled by changing the contents or spacing of the waste package, if the heat output is known, or by changing the surface storage period.

Model sensitivity

The software program used for this work, PLAXIS (Plaxis, 2015), has a new thermo-hydro-mechanical ability and was mainly designed for shallow subsurface soils. It was noted during use that, while the temperature was very reliable, the pore pressures exhibited some differences between software editions (~5%). It is thought that this was due to the low flow rates (due to the low permeability of Boom Clay) and the accuracy of the water flux, although this is not certain. The impact of this was changes in the plastic zones, which could be large, as can be seen in the results in the next chapter. The results reported in this study were undertaken using Plaxis 2015.02 Build 5029.

4.6. Conclusions

The heat output, while not yielding significant temperatures in absolute terms, and in particular, not high enough to change the clay minerology, is likely to cause significant coupled hydro-mechanical processes. In particular, excess pore pressures will be induced, which will not be able to easily dissipate due to the low permeability of the Boom Clay. These pore pressures will reduce the effective stress, which is likely to cause the Boom Clay to yield plastically and increase the damaged zone around the repository tunnels. This has two main impacts: increasing the total stresses and moments applied on the tunnel lining and damaging the Boom Clay, probably increasing the permeability. The first is not anticipated to affect the feasibility of the repository, but should be taken into account during the design of the liner and in terms of the impact on the retrievability of the waste. The potential increase in permeability should be taken into account when assessing the performance of the repository.

5. Sensitivity analysis

5.1. Introduction

In this section a sensitivity analysis is undertaken. In the Netherlands no specific site for the repository has been chosen and, alongside limited experimental data, the conditions of the disposal facility and the behaviour of Boom Clay during the excavations and shortly after the emplacement of heat-producing waste containers are not fully known. In order to assess the relative impact of processes and parameters on the behaviour of Boom Clay under these conditions, a sensitivity analysis has been performed. The aim of this analysis is to understand which properties or conditions mostly affect the system behaviour.

5.2. Cases investigated

The base-case analysis chosen was the Scenario Mid from Chapter 4 and all parameters except for the one varied in each case are kept constant. All the parameters in the cases investigated are chosen based upon the range of values observed in literature. The hydraulic conductivity and thermal expansion coefficient are the two main thermo-hydraulic properties that have not been already varied in Chapter 4, so these are investigated here. The mechanical properties varied are those that were found most sensitive in Arnold et al. (2015). The cases investigated are presented below in Table 5.1.

Table 5.1.: Cases investigated

Parameter	Symb.	Unit	High value	Scenario Mid (see chapter 4)	Low value
Thermal properties					
Thermal expansion coefficient*	α_s	K^{-1}	*3.3x10^{-5}	3.3x10^{-6}	*1.7x10^{-5}
Hydraulic properties					
Hydraulic conductivity	K	m s^{-1}	1x10^{-11}	4x10^{-12}	1x10^{-12}
Mechanical properties					
Effective friction angle	ϕ	°	17.5	12.5	7.5
Effective cohesion	c	MPa	0.7	0.5	0.3
Stiffness* - Reference secant modulus	E_{50}^{ref}	MPa	100	145	190
Initial conditions					
OCR	OCR	-	1.5	2.2	2.7

*The alternative thermal expansion scenarios are both higher.

**All stiffness parameters are assumed to keep the same relationship, i.e. $E_{50}^{ref} = E_{oed}^{ref} = E_{ur}^{ref}/3$.

5.3. Results

The maximum values at any point in the analysis have been taken and compiled in Table 5.2 below.

Table 5.2.: Overview of results

Analysis set variable	Unit		r_{HZ}^{v} (m)*	r_{HZ}^{h} (m)*	$p_{c,\,max}$ (MPa)**	Max. liner hoop stress (kN/m)	Max liner shear force (kN/m)	Max liner moment (kNm / m)
Tunnel only			8.7	9.2	5.8	1 460	46.7	61.0
Base case			13.0	7.2	6.8	3 690	82.0	110.5
Thermal prop.								
		$3.3x10^{-5}$	49.5	fully	9.0	7 446	570.3	558.7
α_s	K^{-1}	$1.7x10^{-5}$	26.5	fully	7.4	5 373	233.0	252.0
		$0.33x10^{-5}$	13.0	7.2	6.8	3 690	82.0	110.5
Hydraulic prop.								
		$1x10^{-11}$	11.8***	6.8	6.6	3 193	73.0	97.8
K	m s^{-1}	$4x10^{-12}$	13.0	7.2	6.8	3 690	82.0	110.5
		$1x10^{-12}$	14.6	7.5	7.1	4 352	101.3	131.8
Mech. prop.								
		17.5	10.8	6.4	6.4	3 004	81.7	99.1
ϕ	°	12.5	13.0	7.2	6.8	3 690	82.0	110.5
		7.5	17.5	8.5	7.4	4 630	81.0	120.0
		0.7	11.3	6.5	6.4	3 047	105.2	119.7
c	MPa	0.5	13.0	7.2	6.8	3 690	82.0	110.5
		0.3	17.0	8.0	7.3	4 372	49.6	89.56
		100	9.5	6.0	6.6	3 723	108.6	130.4
E_{50}^{ref}	MPa	145	13.0	7.2	6.8	3 690	82.0	110.5
		190	15.8	8.2	6.8	3 667	58.7	91.7
Initial cond.								
		1.5	13.8	7.5	6.9	3 723	80.6	109.9
OCR	-	2.2	13.0	7.2	6.8	3 690	82.0	110.5
		2.7	12.4	7.0	6.8	3 662	83.3	111.2

*r_{HZ} is the maximum plastic (hardening) radius, the superscript defines in the horizontal or vertical direction.
** $p_{c,\,max}$ is the maximum cavity pressure
*** plastic zone is below the tunnel only, rest has unloaded

Considering the variation of the model parameters, the most sensitive parameter is seen to be the thermal expansion, α_s. The larger this parameter is, the larger the plastic zone becomes and the greater the stresses and moments on the liner. This means that both the stability and performance of the repository can be significantly affected. The plastic zone development from 32.7 to 35.3 years is shown in Figure 5.1 for $\alpha_s = 3.3x10^{-5}$ K^{-1}. It is seen that, at 35.3 years, almost all of the Boom Clay between the disposal galleries has become plastic, meaning that the Boom Clay around the entire heat producing waste section of the repository could be plastic. As time progresses beyond 35 years this plastic zone then increases in depth until 127 years when the plastic zone is around 100 m thick (50 m above and below the tunnel). The stress on the tunnel at this point is significantly increased to around 9 MPa, which is close to the ultimate strength of the proposed liner with a concrete compressive strength of 45 MPa (~12 MPa, see Figure 4.4 Arnold et al., 2015). The moment applied on the liner also increases from 110 to 560 kNm/m.

This value of thermal expansion is a reasonable value, i.e. not conservative (below that reported by Monfared et al., 2012 and others, see Table 2.1), although above some values reported in literature. Therefore, in agreement with Wiseall et al. (2016), it is recommended that further investigation is undertaken on this parameter. Even by considering a mid-way point between the base case and this minimum value of 1.7x10^{-5} K^{-1}, the plastic zone reaches the full horizontal extent. Additionally, this work considers a linear behaviour of this parameter, whereas the behaviour is known, as a bulk material, to change with OCR, density and stress conditions; therefore further investigation is needed. As mentioned in Chapter 4, the heat output of the spent fuel from the research reactor is not well defined, and this is critical (along with the expansion parameters) to controlling the pore pressures. This heat output can be to some extent controlled by container spacing, although decreasing content may affect the zoning of the repository.

There is relatively little difference between the remaining parameters, with the maximum vertical extent of the plastic zone being 17.0 m and 8.5 m horizontally. The maximum stress on the liner is 7.4 MPa with a maximum moment of 132 kNm/m.

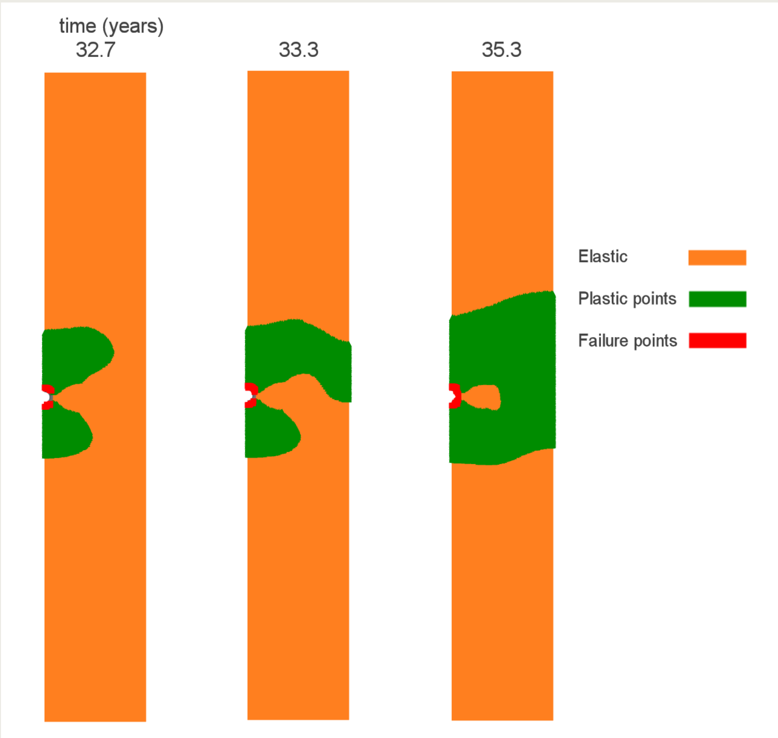

Figure 5.1.: Plastic zone development for case α_s= 3.3x10^{-5} K^{-1}

5.4. Conclusions

As discussed above, there is limited impact on the technical feasibility based on the majority of material parameters varied. However, the thermal expansion of the Boom Clay skeleton is a key parameter which strongly impacts the plastic behaviour of the Boom Clay, potentially yielding a plastic zone which surrounds the entire section of the repository containing heat producing waste, and not isolated to surrounding a single tunnel. This has an impact on the stability of the tunnel lining as well as potential changes in the permeability around the repository.

6. Conclusions and recommendations

This report presents a thermo-hydro-mechanical investigation into the proposed Dutch radioactive waste repository. A selective literature review presented the main THM phenomena expected within Boom Clay. A compilation of properties is given and it is noted that only limited quantitative data on a number of the properties are available.

The computer code, PLAXIS, that utilises of the majority of the temperature dependent properties has been used to simulate the behaviour of Boom Clay, including thermal dilation of water and clay materials, heat conduction and convection, hydraulic flow and mechanical change. The main limitation in terms of material behaviour is that the change in yield surfaces is not represented. It is also noted that this behaviour is not well known experimentally. It is therefore recommended to further investigate this experimentally and the impact on the repository system numerically.

A set of realistic properties were selected and an investigation into the expected behaviour was undertaken. It was seen that the temperature was not significant when evaluated against the limits proposed. The pore pressure was seen to increase, and alongside the thermal expansion of the solid this causes a significant change in the plastic zone around the disposal tunnels. However, neither the extent of the plastic zone nor the increase in stress on the lining were seen to be significant for the material properties selected.

The thermal expansion coefficient for the clay material was seen, in a sensitivity analysis, to be the most sensitive parameter and one which can cause a significant difference in the behaviour of the repository compared to the base scenarios calculated. This can cause a large increase in the plastic zone, so that the plastic zones around the individual tunnels join together to form a large plastic zone. This damages the clay, potentially increasing the permeability, and increases the loads on the tunnel liner. This parameter was also seen in the literature review to not have been measured for Boom Clay extensively, and to have behaviour influenced by other conditions, which makes the experimental interpretation difficult. Therefore it is recommended to further investigate this behaviour both experimentally and subsequently numerically. The long term evolution of the heat output of the waste was based on UOX from a generation II reactor and most of the heat producing waste in the Netherlands is likely to be spent fuel originating from research reactors, and is expected to have a lower heat output than spent fuel from power reactors. This heat output (along with the thermal expansion coefficient) controls the Boom Clay hydro-mechanical response.

The changes in permeability of the Boom Clay around the disposal tunnels due to the potential formation of a plastic zone and change in stress due to the tunnelling and the THM processes are not yet clearly understood. A pore pressure gradient away from the repository is noted during the thermal period which, alongside preferential pathways, could cause transport away from the repository. Since these processes may impact the performance of the repository to some extent they should further be investigated.

It is recommended that all properties are confirmed at depths relevant to the disposal concept in the Netherlands, many have been based upon research undertaken at ~200m depth in Belgium and therefore require confirmation.

References

Arnold, P., P.J. Vardon, M.A. Hicks, J. Fokkens and P.A. Fokker (2015). *A numerical and reliability-based investigation into the technical feasibility of a Dutch radioactive waste repository in Boom Clay, OPERA-PU-TUD311*. Centrale Organisatie Voor Radioactief Afval (COVRA N.V.). url: https://covra.nl/downloads/opera/OPERA-PU-TUD311.pdf.

Baldi, G., T. Hueckel and R. Pellegrini (1988). Thermal volume changes of the mineralwater system in low-porosity clay soils. *Canadian Geotechnical Journal* 25 (4), 807–825. url: http://duke.edu/~hueckel/papers/baldihueckel88.pdf.

Baldi, G., T. Hueckel, A. Peano and R. Pellegrini (1991a). Developments in modelling of thermo-hydro-geomechanical behaviour of Boom clay and clay-based buffer materials (Volume 2), Final report, Report EUR-13365/2. Commission of the European Community. url: http://bookshop.europa.eu/en/developments-in-modelling-of-thermo-hydro-geomechanical-behaviour-of-boom-clay-and-clay-based-buffer-materials-pbCDNB13365/downloads/CD-NB-13-365-EN-C/CDNB13365ENC_001.pdf?FileName=CDNB13365ENC_001.pdf&SKU=CDNB13365ENC_PDF&CatalogueNumber=CD-NB-13-365-EN-C.

— (1991b). Developments in modelling of thermo-hydro-geomechanical behaviour of Boom clay and clay-based buffer materials (Volume 2), Final report, Report EUR-13365/2. Commission of the European Community. url: http://bookshop.europa.eu/en/developments-in-modelling-of-thermo-hydro-geomechanical-behaviour-of-boom-clay-and-clay-based-buffer-materials-pbCDNB13365/downloads/CD-NB-13-365-EN-C/CDNB13365ENC_001.pdf?FileName=CDNB13365ENC_001.pdf&SKU=CDNB13365ENC_PDF&CatalogueNumber=CD-NB-13-365-EN-C.

Boisson, J.-Y. (2005). Clay Club Catalogue of Characteristics of Argillaceous Rocks. OECD Nuclear Energy Agency (NEA), No. 4436. url: http://www.oecd-nea.org/rwm/reports/2005/nea4436-argillaceous-catalogue.pdf.

Bolzon, G. and B.A. Schrefler (2005). Thermal effects in partially saturated soils: a constitutive model. *International Journal for Numerical and Analytical Methods in Geomechanics* 29 (9), 861–877.

Börgesson, L. and J. Hernelind (1999). *Preliminary modelling of the water saturation phase of the buffer and backfill materials*, IPR-00-11, SKB.

Britto, A.M., C. Savvidou, D.V. Maddocks, M.J. Gunn, J.R. Booker (1989). Numerical and centrifuge modelling of coupled heat flow and consolidation around hot cylinders buried in clay, *Géotechnique* 39(1) 13-25.

Cekerevac, C. and L. Laloui (2004). Experimental study of thermal effects on the mechanical behaviour of a clay. *International Journal for Numerical and Analytical Methods in Geomechanics* 28 (3), 209–228.

Chandler, N.A., A.W.L Wan and P.J. Raoch, *The buffer/container experiment design and construction report*. AECL-11792, COG-97-186-I, AECL.

Chen, G.J., T. Maes, F. Vandervoort, X. Sillen, P. Van Marcke, M. Honty, M. Dierick and P. Vanderniepen (2014) Thermal impact on damaged Boom Clay and Opalinus Clay: permeameter and isostatic tests with μCT scanning. *Rock Mechanics and Rock Engineering* 47(1), 87-99.

Chen, G.J., X. Sillen, J. Verstricht and X.L. Li (2011). ATLAS III in situ heating test in Boom Clay: field data, observation and interpretation. *Computers and Geotechnics* 38(5), 683-696.

Chijimatsu, M., T. Fujita, Y. Sugita, K. Amemiya and A. Kobayashi (2001) Field experiment, results and THM behavior in the Kamaishi mine experiment. *International Journal of Rock Mechanics and Mining Science*, 38(1): 67-78.

Coll, C. (2005). Endommagement des Roches Argileuses et Perméabilité Induite au Voisinage D'ouvrage Souterrains. PhD thesis. Grenoble, France: Université Joseph Fourier Grenoble 1. url: http://tel.archives-ouvertes.fr/docs/00/04/84/31/PDF/tel-00010193.pdf.

Collin, F., X.L. Li, J.P. Radu and R. Charlier (2002). Thermo-hydro-mechanical coupling in clay barriers. *Engineering Geology* 64 (2–3), 179–193.

Cui, Y.J., N. Sultan and P. Delage (2000). A thermomechanical model for clays. *Canadian Geotechnical Journal* 37 (3), 607–620.

Cui, Y.-J., T.T. Le, A-M. Tang, P. Delage and X.-L. Li (2009). Investigating the time-dependent behaviour of Boom clay under thermo-mechanical loading. *Géotechnique* 59 (4), 319–329.

De Bruyn, D. and S. Labat (2002). The second phase of ATLAS: the continuation of a running THM test in the HADES underground research facility at Mol. *Engineering Geology* 64 (2–3), 309–316.

De Bruyn, D. and J.-F. Thimus (1996). The influence of temperature on mechanical characteristics of Boom clay: the results of an initial laboratory programme. *Engineering Geology* 41 (1-4),117–126.

Delage, P. (2010). *Deliverable 5: THM Characterisation and Input for Simulation. Thermal Impact on the Damaged Zone Around a Radioactive Waste Disposal in Clay Host Rocks (TIMODAZ)*.

Delage, P. (2013). On the thermal impact on the excavation damaged zone around deep radioactive waste disposal. *Journal of Rock Mechanics and Geotechnical Engineering* 5, 179-190.

Delage, P., N. Sultan and Y.J. Cui (2000). On the thermal consolidation of Boom clay. *Canadian Geotechnical Journal* 37 (2), 343-354.

Deng, Y.F., A.M. Tang, Y.J. Cui, X.P. Nguyen, X.L. Li and L. Wouters (2011a). Laboratory Hydromechanical Characterisation of Boom Clay at Essen and Mol. *Physics and Chemistry of the Earth, Parts A/B/C*, Clays in Natural & Engineered Barriers for Radioactive Waste Confinement 36 (17–18), 1878-1890.

Deng, Y.F., A.M. Tang, Y.J. Cui and X.L. Li (2011b). Study on the hydraulic conductivity of Boom clay. *Canadian Geotechnical Journal* 48 (10), 1461–1470.

Deng, Y.F., Y.J. Cui, A.M. Tang, X.L. Li and X. Sillen (2012). An experimental study on the secondary deformation of Boom clay. *Applied Clay Science* 59–60, 19–25.

Djeran, I., B. Bazargan, A. Giraud and G. Rousset (1994). *Etude expérimental du comportement Thermo-Hydro-Mecanique de l'argile de Boom. Rapport final*. Report No. 94-002. SCK·CEN.

ENRESSA (2000) *FEBEX project: Full-scale engineered barriers experiment for a deep geological repository for high-level radioactive waste in crystalline host rock, Final report*. ENRESSA.

François, B., L. Laloui and C. Laurent (2009). Thermo-hydro-mechanical simulation of ATLAS in situ large scale test in Boom Clay. *Computers and Geotechnics* 36 (4), 626-640.

Galavi (2013) *Groundwater flow, fully coupled flow deformation and undrained analyses in PLAXIS 2D and 3D*. Plaxis. url: http://kb.plaxis.nl/sites/kb.plaxis.nl/files/kb-publications/Galavi_Groundwater_flow_and_Coupled_analysis.pdf.

Garitte, B., A. Gens, J. Vaunat and G. Armand (2012). Thermal Conductivity of Argillaceous Rocks: Determination Methodology Using In Situ Heating Tests. *Rock Mechanics and Rock Engineering* 47 (1), 111–129.

Gens, A., M. Sánchez, L. Do, N. Guimaraes, E.E. Alonso, A. Lloret, S. Olivella, M. V. Villar and F. Huertas (2009). A full-scale in situ heating test for high-level nuclear waste disposal: observations, analysis and interpretation. *Géotechnique* 59 (4), 377–399.

Ghabezloo, S. and J. Sulem (2009). Stress dependent thermal pressurization of a fluid-saturated rock. *Rock Mechanics and Rock Engineering* 42 (1), 1–24.

Habibagahi, K. (1977). Temperature effect and the concept of effective void ratio. *Indian Geotechnical Journal* 1, 14-34.

Hart, J. and A.D. Poley (2014). *Organizing and Structuring the OPERA Research Efforts using Safety Statements, OPERA-PU-NRG2112*. Centrale Organisatie Voor Radioactief Afval (COVRA N.V.). url: https://www.covra.nl/downloads/opera/OPERA-PU-NRG2112-SafetyStatements_EA.pdf.

Horseman, S.T. and T.J. McEwen (1996). Thermal constraints on disposal of heat-emitting wastein argillaceous rocks. *Engineering Geology* 41 (1–4), 5–16.

Horseman, S.T., M.G. Winter and D.C. Entwistle (1987). Geotechnical Characterization of Boom Clay in Relation to the Disposal of Radioactive Waste. Commission of the European Communities.

Horseman, S.T., M.G. Winter and D.C. Entwistle (1993). Triaxial experiments on Boom Clay. In: *The Engineering Geology of Weak Rock*. Balkema, Rotterdam, 36–43.

Hueckel, T. and G. Baldi (1990). Thermoplasticity of Saturated Clays: Experimental Constitutive Study. *Journal of Geotechnical Engineering* 116 (12), 1778–1796.

Hueckel, T. and R. Pellegrini (1992). Effective stress and water pressure in saturated clays during heating-cooling cycles. *Canadian Geotechnical Journal* 29 (6), 1095–1102. url: http://duke.edu/~hueckel/papers/cooling_cycles_failure.pdf.

Hueckel, T., B. François and L. Laloui (2009) Explaining thermal failure in saturated clays. *Géotechnique* 59 (3) 197-212.

Kaye, G.W.C. and T.M. Laby, T.M. (1973). *Tables of physical and chemical constants*, 14th Edition, Longmans, London.

Laloui, L. (1993). *Modélisation du comportement thermo-hydro-mécanique des milieux poreux anélastique*. PhD thesis. Ecole Centrale de Paris.

Lê, T.T. (2008) *Thermo-hydro-mechanical- behaviour of Boom clay*. PhD thesis. Ecole des Ponts ParisTech.

Li, X., F. Bernier, T. Vietor and P. Lebon (2007). Deliverable 2: State of the art THMC. Thermal Impact on the Damaged Zone Around a Radioactive Waste Disposal in Clay Host Rocks (TIMODAZ). url: http://www.timodaz.eu/deliverables.aspx?dwnld=TIMODAZD2formatECfinal.doc&itemid=bc9c5d91-17e1-4cec-929c-2c8a49ff777f&id=WP2.

Lima, A., E. Romero, A. Gens, J. Muñoz and X. L. Li (2009). Heating Pulse Tests under Constant Volume on Natural Boom clay. In: *International Symposium on Unsaturated Soil Mechanics and Deep Geological Nuclear Waste Disposal (UNSAT-WASTE 2009)*. Shanghai, 136–141. url: http://upcommons.upc.edu/e-prints/bitstream/2117/9922/1/PosterLuxembourg_LRVGL_THMC_P60Lima\%20et\%20al.pdf.

Meeussen, J.C.L. and E. Rosca-Bocancea (2014). Determination of the inventory, Part B: Matrix composition, OPERA-PU-NRG112B. Centrale Organisatie Voor Radioactief Afval (COVRA N.V.) url: https://covra.nl/downloads/opera/OPERA-PU-NRG1112B.pdf.

Mitchell, J.K. and Soga K. (2005) *Fundamentals of soil behaviour*. 3rd Edition. Wiley.

Monfared, M., J. Sulem, P. Delage, M. Mohajerani (2012) On the THM behaviour of a sheared Boom clay sample: Application to the behaviour and sealing properties of the EDZ, *Engineering Geology* 124, 47-58.

Morin, R. and A.J. Silva (1984). The effect of high pressure and high temperature on some physical properties of ocean sediments. *Journal of Geophysical Research* 89, 511–526.

Noorishad, J., C.F. Tsang and P.A. Witherspoon (1984). Coupled thermal-hydraulic-mechanical phenomena in saturated fractured porous rocks: Numerical approach. *Journal of Geophysical Research* 89 (B12) 10365-10373.

Olivella, S., A. Gens, J. Carrera and E.E. Alonso (1995). Numerical formulation for a simulator (CODE BRIGHT) for the coupled analysis of saline media. *Engineering Computations*, 13(7), 87-112.

Olivella, S., A. Gens (2005) Double structure THM analyses of a heating test in a fractured tuff incorporating intrinsic permeability variations. *International Journal of Rock Mechanics and Mining Sciences*, 42 (5-6), 667-679.

ONDRAF/NIRAS (2001a). *SAFIR 2 - Safety Assessment and Feasibility Interim Report 2*. Belgian agency for radioactive waste and enriched fissile materials, NIROND 2001-06 E.

— (2001b). *Technical overview of the SAFIR 2 report - Safety Assessment and Feasibility, Interim Report 2*. Belgian agency for radioactive waste and enriched fissile materials, NIROND 2001-05 E.

Onofrei, C. and M. Gray (1996). Modelling hygro-thermo-mechanical behaviour of engineered clay barriers: validation phase. *Engineering Geology 41 (1), 301-318*.

Picard, J.-M. (1994). *Écrouissage thermique des argiles saturées: application au stockage des déchets radioactifs*. PhD thesis. École Nationale des Ponts et Chaussées. url: http://pastel.archives-ouvertes.fr/docs/00/57/40/24/PDF/1994TH_PICARD_JM_NS18466.pdf.

Plaxis (2015). *Thermal and coupled THM analysis*. Plaxis. url: http://kb.plaxis.nl/publications/thermal-and-coupled-thm-analysis.

Rijkers, R.H.B., D.I. Huisman, G. de Lang, J.P. Weijers and W. Witmans-Parker (1998). Inventarisatie geomechanische, geochemische en geohydrologische eigenschappen van Tertiaire kleipakketten CAR Fase II - Eindrapport. Nederlands Instituut vor Toegepaste Geowetenschappen (TNO). url: http://www.covra.nl/cms-file/get/iFileId/2475.

Rutqvist, J., L. Börgesson, M. Chijimatsu, A. Kobayashi, L. Jing, T.S. Nguyen, J. Noorishad and C.-F. Tsang (2001). Thermohydromechanics of partially saturated geological media: governing equations and formulation of four finite element models. *International Journal of Rock Mechanics & Mining Sciences* 38, 105-127.

Sillen, X. and J. Marivoet (2007). *Thermal impact of a HLW repository in clay, Deep disposal of vitrified high-level waste and spent fuel*, External report SCK·CEN-ER-38. SCK·CEN.

Smith, P., B. Cornélis, M. Capouet, M. van Geet (2009) *The long-term safety strategy for the geological disposal of radioactive waste, SFC1 level 4 report: second full draft, NIROND-TR-2009-12E*,ONDRAF/NIRAS.

Sultan, N. (1997). Etude du comportement thermo-mécanique de l'argile de Boom: expériences et modélisation. PhD thesis. Paris, France: École Nationale des Ponts et Chaussées.

Sultan, N., P Delage and Y.J Cui (2002). Temperature effects on the volume change behaviour of Boom clay. *Engineering Geology* 64 (2-3), 135–145.

Sultan, N., Y.-J. Cui and P. Delage (2010). Yielding and plastic behaviour of Boom Clay. *Géotechnique* 60 (9), 657–666.

Towhata, I., Kuntiwattanakul, P., Seko, I. and Ohishi, K. (1993). Volume change of clays induced by heating as observed in consolidation tests. *Soils and Foundations* 33 (4), 170-183.

Thomas, H.R. and Y. He (1998). Modelling the behaviour of unsaturated soil using an elasto plastic constitutive relationship", *Géotechnique*, 48(5), 589-603.

Thomas, H.R., P.J. Vardon and P.J. Cleall (2014). Three-dimensional behavior of a prototype radioactive waste repository in fractured granitic rock, *Canadian Geotechnical Journal* 51(3), 246-259, doi: 10.1139/cgj-2013-0094.

Van Marcke, P. and B. Laenen (2005). *The Ypresian clay as possible host rock for radioactive waste disposal: An evaluation*. NIROND TR-2005-01. ONDRAF/NIRAS.

Vandenberghe, N. and W. Fock (1989). Temperature data in the subsurface of Belgium. *Tectonophysics* 164 (2-4), 237–250.

Vardoulakis, I. (2002). Dynamic thermo-poro-mechanical analysis of catastrophic landslides. *Géotechnique* 52 (3), 157–171.

Verhoef, E.V., E.A.C. Neeft, G. Deissmann, A. Filby, R.B. Wiegers and D.A. Kers (2016). Waste families in OPERA, OPERA-PG-COV023. Centrale Organisatie Voor Radioactief Afval (COVRA N.V.). url: https://www.covra.nl/downloads/opera/OPERA-PG-COV023.pdf.

Verhoef, E., E. Neeft, J. Grupa and A. Poley (2014). *Outline of a disposal concept in clay, OPERA-PG-COV008, First update*. Centrale Organisatie Voor Radioactief Afval (COVRA N.V.). url: https://www.covra.nl/downloads/opera/OPERA-PG-COV008_rev1.pdf.

Volckaert, G., L. Ortiz, P. De Canniére, M. Put, S.T. Horseman, J.F. Harrington, V. Fioravante and M. Impey (1995). MEGAS – Modelling and experiments on gas migration in repository host rocks, Final report - Phase 1, Report EUR 17453 EN. Luxenbourg: Commission of the European Comunity. url: http://bookshop.europa.eu/en/megas-pbCGNA16235/downloads/CG-NA-16-235-EN-C/CGNA16235ENC_001.pdf?FileName=CGNA16235ENC_001.pdf&SKU=CGNA16235ENC_PDF&CatalogueNumber=CG-NA-16-235-EN-C.

Weetjens, E. (2009). *Update of the near field temperature evolution calculations for disposal of UNE-55, MOX-50 and vitrified HLW in a supercontainer- based geological repository*. SCK·CEN-ER-86, SCK. ·CEN url: http://publications.sckcen.be/dspace/bitstream/10038/1039/1/er_86.pdf.

Yu, L., E. Weetjens, X. Sillen, T. Vietor, X.L. Li, P. Delage, V. Labiouse and R. Charlier (2014). Consequences of the thermal transient on the evolution of the damaged zone around a repository for heat-emitting high-level radioactive waste in a clay formation: a performance assessment perspective. *Rock Mechanics and Rock Engineering* 47(1), 3–19. doi:10.1007/s00603-013-0409-4.

Wiseall A., C. Graham, S. Zihms, J. Harrington, R. Cuss, S. Gregory, R. Shaw (2016) *Properties and behaviour of the Boom Clay formation within a Dutch repository concept. Draft*. Centrale Organisatie Voor Radioactief Afval (COVRA N.V.)

OPERA

Meer informatie:

Postadres
Postbus 202
4380 AE Vlissingen

T 0113-616 666
F 0113-616 650
E info@covra.nl

www.covra.nl